


DetectEV: A functional enzymatic assay to assess integrity and bioactivity of extracellular vesicles

Giorgia Adamo¹  | Sabrina Picciotto¹ | Paola Gargano¹ | Angela Paterna² |
Samuele Raccosta² | Estella Rao² | Daniele Paolo Romancino¹ | Giulio Gherzi³ |
Mauro Manno² | Monica Salamone¹ | Antonella Bongiovanni¹

¹Cell-Tech HUB and Institute for Research and Biomedical Innovation (IRIB), National Research Council of Italy (CNR), Palermo, Italy

²Cell-Tech HUB and Institute of Biophysics (IBF), National Research Council of Italy (CNR), Palermo, Italy

³Department of Biological, Chemical and Pharmaceutical Sciences and Technologies (STEBICEF), University of Palermo, Palermo, Italy

Correspondence

Giorgia Adamo and Antonella Bongiovanni, Cell-Tech HUB and Institute for Research and Biomedical Innovation (IRIB), National Research Council of Italy (CNR), Palermo, Italy. Email: giorgia.adamo@irib.cnr.it and antonella.bongiovanni@irib.cnr.it

Funding information

MUR PNRR "National Center for Gene Therapy and Drugs based on RNA Technology, Grant/Award Number: CN00000041 CN3 RNA; Consiglio Nazionale delle Ricerche, Grant/Award Number: @IRIB2023; European Union's Horizon 2020 research and innovation programme, Grant/Award Numbers: 801338, 952183

Abstract

The application of extracellular vesicles (EVs) as therapeutics or nanocarriers in cell-free therapies necessitates meticulous evaluations of different features, including their identity, bioactivity, batch-to-batch reproducibility, and stability. Given the inherent heterogeneity in EV preparations, this assessment demands sensitive functional assays to provide key quality control metrics, complementing established methods to ensure that EV preparations meet the required functionality and quality standards. Here, we introduce the detectEV assay, an enzymatic-based approach for assessing EV luminal cargo bioactivity and membrane integrity. This method is fast, cost-effective, and quantifiable through enzymatic units. Utilizing microalgae-derived EVs, known as nanoalgsomes, as model systems, we optimised the assay parameters and validated its sensitivity and specificity in quantifying the enzymatic activity of esterases within the EV lumen while also evaluating EV membrane integrity. Compared to conventional methods that assess physicochemical features of EVs, our single-step analysis efficiently detects batch-to-batch variations by evaluating changes in luminal cargo bioactivity and integrity across various EV samples, including differences under distinct storage conditions and following diverse isolation and exogenous loading methods, all using small sample sizes. The detectEV assay's application to various human-derived EV types demonstrated its versatility and potential universality. Additionally, the assay effectively predicted EV functionality, such as the antioxidant activity of different nanoalgsome batches. Our findings underscore the detectEV assay's utility in comprehensive characterization of EV functionality and integrity, enhancing batch-to-batch reproducibility and facilitating their therapeutic applications.

KEYWORDS

bioactivity, extracellular vesicles, functional enzymatic assay, integrity, quality check, standardization

Giorgia Adamo and Sabrina Picciotto contributed equally to this study.

This is an open access article under the terms of the [Creative Commons Attribution-NonCommercial-NoDerivs License](https://creativecommons.org/licenses/by-nc-nd/4.0/), which permits use and distribution in any medium, provided the original work is properly cited, the use is non-commercial and no modifications or adaptations are made.

© 2025 The Author(s). *Journal of Extracellular Vesicles* published by Wiley Periodicals LLC on behalf of International Society for Extracellular Vesicles.

1 | INTRODUCTION

Extracellular vesicles (EVs) are essential signalling mediators involved in intercellular and inter-organism communications (Adamo et al., 2021; Raposo & Stoorvogel, 2013; Yáñez-Mó et al., 2015). EV-based signalling depends on their lumen, membrane-integral or -associated cargo, which may be naturally-sourced (e.g., bioactive molecules such as enzymes) or be exogenously loaded (e.g., therapeutic molecules) (Chen, Zhao et al., 2021; O'Grady et al., 2022). In recent years, EVs have come to be considered one of the most promising innate effectors for cell-free therapy and bio-nanovehicles for drug delivery (Herrmann & Wood, 2021; Sun et al., 2021). However, despite the advances in the field, many challenges with EV-based therapies still stand (Herrmann & Wood, 2021). The therapeutic efficacy of EVs depends on their intrinsic properties, including the membrane stability (Russel et al., 2019). To validate the quality of EV preparations for therapeutic application and define the 'Critical Quality Attributes', EV-inherent features should be tested to qualify them as suitable for subsequent clinical functional testing applications (Nguyen et al., 2020; Yekula et al., 2020). In this view, to achieve an adequate assessment of EV bioactivity, appropriate functional assays need to be created to support common EV-related biophysical and biochemical quality controls (QCs).

Ideally, specific functional assays would predict whether a particular EV-preparation holds the potential to achieve its intended therapeutic effects or its 'potency,' which could be further investigated in a 'formal disease-specific' potency assays (Nguyen et al., 2020).

The MISEV-2023 guidelines and the EV-TRACK knowledgebase propose and support rigorous procedures required to document specific EV-associated functional activities to cope with the advance of EV research, assuring and improving the quality of these studies (Van Deun et al., 2017; Welsh et al., 2024). In particular, the MISEV-2023 recommendations for conducting functional studies encourage researchers to conduct dose-response and time-course studies, incorporate EV-negative controls, utilise EVs from different cell types for comparative analysis, and employ treated-EV samples to differentiate EV-specific effects from co-isolating materials. Moreover, it is suggested to explore the impact of EV separation or storage methods on EV activity to optimise experimental conditions (Welsh et al., 2024).

Furthermore, a functional assay should be simple and sensitive enough using a low amount of EV samples to facilitate the following studies (Gimona et al., 2021; Pachler et al., 2017). To date, only few *in vitro* and *in vivo* assays have been used to interrogate the potency of specific types of EVs; however, many of them failed for several challenges that make reliable assays difficult to set up (Nguyen et al., 2020; Ramirez et al., 2018). In the field of EVs, it is expected that no single test can adequately measure all product attributes that can predict clinical efficacy. Further, the development of ubiquitous, standardisable and functional test for evaluating the bioactivity can be tricky for EVs because they are highly heterogeneous and show different bioactivity and biomolecular signatures (Ramirez et al., 2018). Despite this evidence, there is a need for a precise procedure to accurately qualify EV preparations, which can be applied to various types of EVs, regardless of their origin or preparation method (Gimona et al., 2021; LeClaire et al., 2021). It would be advisable to identify a common feature among vesicles that could predict EV functionality. An example could be evaluating the EV membrane integrity by measuring luminal enzymatic activity. In this context, a fascinating and unexplored aspect is the presence of a class of enzymes ubiquitously present in EVs: esterases within EVs. Indeed, our search of the publicly available ExoCarta database revealed a noticeable and extremely robust association between esterase-like enzymes and vesicle-cargo proteins in EVs derived from many sources, including those of mammalian origin (mice, rats, and cows), several human body fluids (blood, saliva, and urine), and numerous human cancer and normal cell lines (more than 60 hits for 'esterase' from the ExoCarta database, <http://www.exocarta.org>) (Gonzales et al., 2009; Gonzalez-Begne et al., 2009; Simpson et al., 2012). Furthermore, many recent proteomic analyses described the presence of esterase-like enzymes in EVs isolated from bacteria (like *Escherichia coli* and *Pseudomonas aeruginosa*), plants and fungi (*Candida albicans* and *Aspergillus fumigatus*) (Bleackley et al., 2020; Choi et al., 2011; Garcia-Ceron et al., 2021; McMillan & Kuehn, 2022; Pocsfalvi et al., 2018; Rizzo et al., 2020). A large number of enzymes, such as choline esterases, carboxylic ester hydrolases, lipases, and proteases, are member of the esterase' superfamily, catalysing the cleavage of ester bonds (Cygler et al., 1993). The measure of esterase activity can be performed by employing an enzymatic assay, using specific substrate, like the fluorescein diacetate (FDA). FDA (i.e., 3'-6'-diacetyl-fluorescein, FDA) is a non-fluorescent fluorescein molecule conjugated to two acetate radicals (Adam & Duncan, 2001). This is a fluorogenic ester compound able to pass through phospholipid bilayers, like plasma and EV membranes. Indeed, when inside cells or EVs, FDA is hydrolysed by non-specific esterases to produce a negatively charged membrane-impermeable green fluorescent molecule (i.e., fluorescein) (Fontvieille et al., 1992). This membrane-permeable esterase substrate is commonly used as a probe to study microbial metabolic activity or to monitor the cell viability of fungi, plants, microalgae, and bacteria. It can be used both to measure enzymatic activity, essential for activating its fluorescence, and to evaluate membrane integrity, necessary for the intracellular or intra-vesicular retention of its fluorescent product (Ender et al., 2020; Gray et al., 2015).

In the EV-field, different approaches have described the use of membrane-permeant enzymatic substrates to label EVs, including carboxyfluorescein diacetate succinimidyl ester (CFSE), and calcein acetoxymethyl ester (calcein-AM) (de Rond et al., 2018; Ender et al., 2020; Kormelink et al., 2016; Nikiforova et al., 2021; Pospichalova et al., 2015; Tertel et al., 2022). Similarly to FDA, these molecules are cleaved by esterases, which are present inside cells as well as in secreted EVs (Gray et al., 2015). These experimental approaches have been developed to make EV fluorescent and detectable for flow cytometry applications or for fluorescent

microscopy; however, these methods are not quantitative and do not directly provide information on EV-functional quality (Morales-Kastresana et al., 2017).

In this study, we introduced the detectEV assay as a new, simple, highly sensitive and precise functional test, able to define EV integrity and identity, by evaluating the EV-associated enzymatic activity, using a FDA-based enzymatic method (Adam & Duncan, 2001; Sirt Çıplak & Akoğlu, 2020). Throughout this assay, we considered various aspects crucial for working with EVs, as comparing the quality of different EV batches or EVs isolated using different methods (differential ultracentrifugation, dUC, versus tangential flow filtration, TFF). Additionally, we assessed the luminal enzymatic bioactivity and integrity of EVs stored under different conditions or manipulated using various physical loading techniques, using the proposed functional test and comparing these results with a standard method for EV evaluations, like nanoparticle tracking analysis (Welsh et al., 2024). Finally, we proved that the detectEV assay can predict the functionality of different preparations of EVs. The versatility of the detectEV assay for different type of EVs, including human ones, encouraged its application as functional enzymatic assay for rapid quality check (QC) of EVs, as in a single step analysis giving two important pieces of information: the bioactivity of a luminal molecules that is related to membrane integrity of EV preparations.

2 | RESULTS

2.1 | Set up of the detectEV assay

To set up the detectEV assay, we used microalgae-derived EVs (known as nanoalgsomes or algsomes) as small EV (sEV) models (Adamo et al., 2021; Picciotto et al., 2022). We isolated nanoalgsomes from the conditioned media of *Tetraselmis chuii* microalgae, both in small and large scale using dUC and TFF methods, respectively. Next, we characterised them by evaluating selected MISEV-2023 quality parameters (Adamo et al., 2021; Welsh et al., 2024). These included biophysical characterization of size distribution and morphology by dynamic light scattering, nanoparticle tracking analysis (NTA) and atomic force microscopy (AFM), and a biochemical characterization of protein content using bicinchoninic acid assay (BCA assay) and immunoblot (IB) analysis for EV-biomarkers (Adamo et al., 2021; Paterna et al., 2022). Data relative to nanoalgsome characterization are reported in Figure S1 (EV-TRACK ID: EV231004). In particular, nanoalgsomes exhibited a monodisperse size distribution of approximately 100 ± 10 nm, a rounded and homogeneous morphology, and the presence of enriched EV biomarkers such as Alix, H⁺-ATPase, and β -actin. Additionally, they are expected to demonstrate an appropriate EV particle number/protein ratio, in which 1 μ g of total EV protein corresponding to a range of $5 - 10 \times 10^9$ particles (Sverdllov, 2012).

In the proof-of-concept of the proposed detectEV assay, the accumulation of fluorescein inside EVs is a measure of two independent parameters: enzymatic activity and membrane integrity (Figure 1a). Therefore, in a first pilot test, we incubated a fixed amount of nanoalgsomes (2×10^{10}) with FDA (35 μ mol) in 200 μ L of phosphate-buffered saline (PBS) solution and checked for fluorescence emission with respect to EV-negative control (nanoalgsome vehicle solution, i.e., PBS), using spectrofluorometer readings (Figure 1b). The fluorescence emission was detected over time, up to 16 h (960 min). Interestingly, we got a rapid time-dependent increase of fluorescence intensity only in the nanoalgsome samples compared to the negative control. The trend of fluorescence increase over time exhibits a direct proportionality, that is, a linear relationship up to 8 h, and subsequently reaches a plateau after approximately 15 h, probably due to substrate depletion or enzyme inactivation (Figure 2a).

Based on this result, fundamental parameters such as the temperature set at 22°C (i.e., room temperature) and the duration of the assay limited to 3 h (a time frame during which the reaction remains within the exponential phase and exhibits a linear trend) were defined. These parameters were established to ensure the test is rapid and sufficiently sensitive.

2.2 | Validation of the quantitative FDA-based functional enzymatic assay for EVs

For the validation of the analytical procedure, it is important to establish key parameters such as specificity, accuracy, and precision. Initially, we gated the appropriate approach to develop a functional assay for EVs that provides a universally quantifiable and standardizable read out. To accomplish that we had to determine the amount of FDA that is enzymatically cleaved during the assay, establishing a calibration curve to interpolate unknown quantities of cleaved FDA. Therefore, the fluorescein, corresponding to the reaction product of FDA hydrolysis, was deemed a reliable choice, and, in turn, it was generated a standard calibration curve using it (Dzionic et al., 2018). Figure 2b illustrates **the calibration curve** derived from serial dilutions of a fluorescein stock solution, where the fluorescence emission intensity exhibits a direct correlation with fluorescein concentration. The resulting calibration curve demonstrates a linear trend, facilitating the straightforward conversion of fluorescence intensity emitted following the enzymatic reactions (i.e., FDA hydrolysis by active EV-related esterases) into nanomole (nmol) of produced fluorescein. Furthermore, in the development of the detectEV assay, we have chosen to adopt the enzymatic units (U) to quantitatively assess EV-related enzymatic activity. This because the specific enzymatic activity is universally expressed as U,

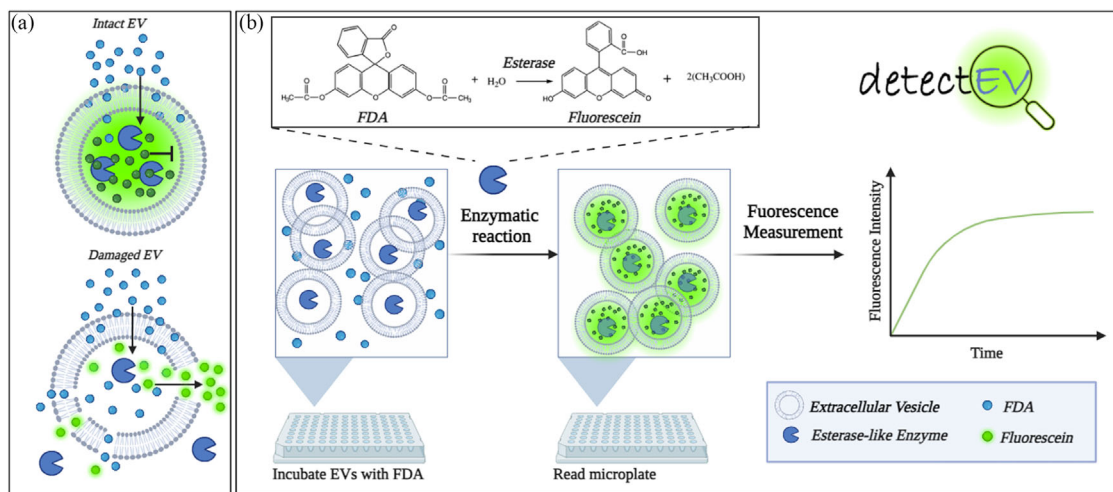


FIGURE 1 Schematic representation of the detectEV assay for evaluating the bioactivity and integrity of extracellular vesicles. (a) Graphic representation of FDA feature in intact and damaged EVs. Intact EVs (top) retain their luminal contents, including esterase-like enzymes and the produced-fluorescein molecules, within the membrane, while damaged EVs (bottom) have compromised membranes leading to the leakage of their cargo contents. (b) Overview of the detectEV assay procedure. EVs are incubated with fluorescein diacetate, which penetrates the vesicles. Inside intact EVs, esterase-like enzymes hydrolyse fluorescein diacetate to produce fluorescein, a fluorescent compound that is membrane impermeable. The enzymatic reaction's mechanism is shown in the inset, indicating the hydrolysis of fluorescein diacetate to fluorescein and acetic acid. After the EV incubation with fluorescein diacetate substrate, the fluorescence intensity is measured using a microplate reader (excitation 488 nm, emission 520 nm). The fluorescence intensity over time is depicted in the graph on the right, showing the expected increase in fluorescence as the enzymatic reaction proceeds. Created with [BioRender.com](https://www.biorender.com). EV, extracellular vesicle; FDA, fluorescein diacetate.

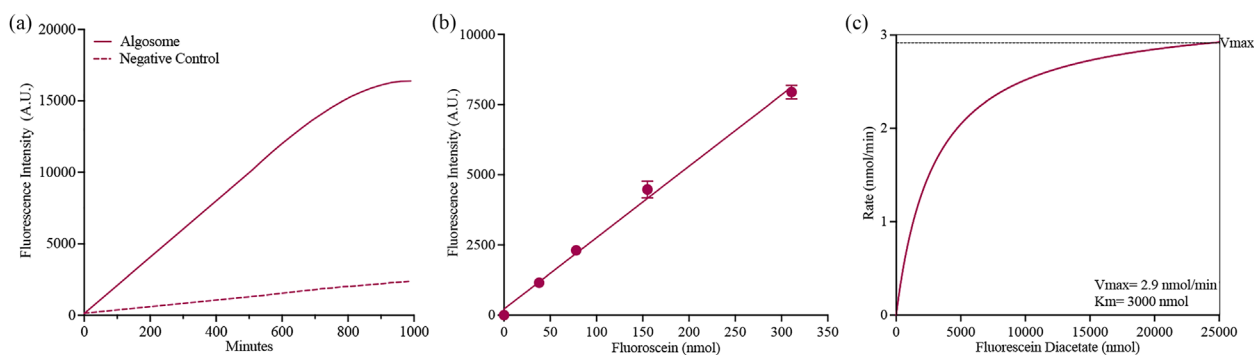


FIGURE 2 Set up and validation of the detectEV assay. (a) Time-dependent increase in fluorescence intensity of microalgal-derived extracellular vesicles incubated with fluorescein diacetate. The fluorescence intensity expressed as arbitrary unit, AU (excitation 488 nm, emission 520 nm) of a representative microalgal-derived extracellular vesicles (i.e., nanoalgosomes or algosomes) sample incubated with fluorescein diacetate shows a significant increase over time, indicating the presence of esterase activity and intact vesicles. In contrast, the negative control (PBS, nanoalgosome vehicle control) shows minimal fluorescence intensity, confirming the specificity of the fluorescence signal to the enzymatic activity of the vesicles. (b) Setting up of the detectEV assay. Calibration curve of fluorescein, depicting the linear relationship between fluorescence intensity and the concentration of fluorescein (nmol). Error bars represent the standard deviation of the mean fluorescence intensity of independent readings ($n = 3$). (c) Michaelis–Menten graph illustrating the enzymatic cleavage rate of fluorescein diacetate (nmol/min) catalysed by nanoalgosome enzymes. The curve demonstrates the relationship between the rate of reaction and the concentration of fluorescein diacetate (nmol). The maximum reaction rate (V_{max}) is 2.9 nmol/min, and the Michaelis constant (K_m) is 3000 nmol.

representing the quantity of enzyme required to catalyse the conversion of one nanomole of substrate into product per minute (nmol/min), under the specified conditions of the assay method (Robinson, 2015).

Therefore, within the detectEV setup, enzymatic units (nmol/min) will be determined by utilizing a calibration curve of free fluorescein to calculate the total nmols generated over 180 min. Subsequently, total nmols will be divided by the overall time (180 min) to yield the final readout in nmol/min.

Additionally, in order to determine kinetic parameters of the enzymatic reaction, we performed an enzymatic kinetic study at increasing substrate concentrations, to measure the reaction rate (i.e., the amount of substrate converted to product per unit of time) at constant nanoalgosome concentrations (2×10^{10} nanoalgosomes). This approach reflects the Michaelis–Menten model, a widely utilised method for studying enzyme kinetics (Bisswanger, 2014; Choi et al., 2017; Michaelis et al., 2011). As shown in Figure 2c, by plotting reaction rates against the respective substrate concentration, we obtained a canonical hyperbolic

relationship, through which it was possible to derive kinetic parameters, including the maximum reaction velocity (V_{\max} , equal to 2.9 nmol/min) and the kinetic constant (as Michaelis constant, K_m equal to 3 μmol) (Michaelis et al., 2011; Duggleby & Wood, 1989).

These values could give an indication on the substrate concentration to be used to ensure that the enzymes are acting near V_{\max} (Bisswanger, 2014). Typically, a substrate concentration higher than the K_m value is employed in enzymatic activity studies (Bisswanger, 2014). Based on this evidence, for establishing the right detectEV assay condition, we decided to fix the substrate concentration (i.e., FDA) at 6 times the K_m that is at 18 μmol (Michaelis et al., 2011; Duggleby, 1979).

2.3 | Analytical sensitivity and specificity of detectEV assay

To establish the **analytical sensitivity** of the detectEV assay, we determined the limit of detection (LOD) by conducting a dose-response test to identify the lowest concentration of EVs that could be distinguished from the background noise. This background noise corresponds to the nanoalgaosome buffer control (v/v of PBS solution) incubated with FDA.

Therefore, to determine the LOD, we incubated different nanoalgaosome concentrations of the same preparation batch (ranging from 3×10^8 to 2×10^{10} EVs) with 18 μmol of FDA. We found that the enzymatic assay is EV-dose responsive, with the minimum detection limit of 2×10^9 nanoalgaosomes (Figure 3a). Moreover, to assess potential influence of FDA auto-hydrolysis in different media, background fluorescence measurements were performed (Figure S2a–b). FDA auto-hydrolysis was tested in microalgal F/2 medium and in human cell culture media (i.e., complete Dulbecco's Modified Eagle Medium, DMEM with high and low glucose supplemented with EV-depleted serum), both in their original formulation and their post-purification form (using tangential flow filtration and differential ultracentrifugation). These controls ensured that any observed fluorescence was due to EV functionality rather than auto-hydrolysis of the FDA substrate. Figure S2b shows the background fluorescence measurements of the FDA up to 180 min: in F/2 medium, no significant auto-hydrolysis was observed, both in the original medium and the post-purification form. Conversely, both original formulation of DMEM media analysed (with high and low glucose) exhibited a high background signal, indicating significant FDA auto-hydrolysis, rendering the detectEV assay inapplicable for EVs in conditioned media like DMEM, as the high background could mask EV enzymatic activity-derived signals. While, FDA auto-hydrolysis of these post-isolation forms gave a signal comparable to the negative control (i.e., PBS ranged from 400 to 800 arbitrary units of fluorescence), corroborating the robustness of the measurements. Consequently, all the detectEV-related experiments were conducted with EVs isolated and resuspended in PBS.

Additionally, to verify whether the **analytical specificity** of the detectEV assay is associated with the bioactivity of active enzymes within intact EVs, we utilised nanoalgaosomes treated with varying concentrations of a non-ionic detergent (Triton-X 100 at 0.1%, 0.25%, 0.5%, and 1%). This detergent permeabilises lipid membrane bilayers and gently solubilises proteins while maintaining their activity, including enzymatic activity (Jamur & Oliver, 2010; Perna et al., 2017). As established in our prior study, complete nanoalgaosome lysis was induced by treating with 1% Triton-X 100 (Adamo et al., 2021). Subsequently, we performed the detectEV assay using detergent-treated nanoalgaosomes respect to not treated ones. The results showed in Figure 3b revealed higher enzymatic activity in the intact/no-treated nanoalgaosomes, while this activity decreased with increasing doses of detergent, reaching no activity at the critical detergent concentration of 1%. This suggests that the measurable fluorescent signal relies on active esterases within the physiological environment of intact EVs. Identical results were observed when EVs were lysed, and proteins were denatured by boiling at 100°C for 10 min, thereby confirming the specificity of the proposed functional assay (Figure 3b).

Furthermore, to corroborate these results, we followed the enzymatic kinetics of nanoalgaosomes treated with 1% Triton-X 100 after established time points (i.e., after 1, 2, and 3 h from the addition of the FDA substrate). As illustrated in Figure 3c, the fluorescence intensity was measured every 15 min during this time course test and, as expected, each no-treated sample exhibited a similar trend, namely a linear increase in fluorescence intensity over time. However, this increase ceased upon the addition of 1% Triton-X 100, remaining quite constant until the end of the assay. This trend demonstrates that the fluorescence intensity, corresponding to produced fluorescein, is correlated with membrane integrity of EVs. Indeed, when EVs are lysed the enzymatic reaction halts. Furthermore, the fluorescence values of fluorescein remain quite constant in intact vesicles compared to the respective lysed vesicles over time and for each condition, thereby validating the accurate application of the previously described calibration curve for free fluorescein, which is utilised in calculating nmols of fluorescein produced during the assay. Moreover, to corroborate the specificity of the detectEV assay, we performed a protease pre-treatment to verify that the quantified bioactivity is related to esterases located in the EV lumen. For this EV-protease treatment 0.25% trypsin was added to the EV samples and incubated at 37°C for 15 min (Chen, Sun et al., 2021). By setting of the proper washing procedures, we successfully removed trypsin molecules from EV samples, checking also the proper nanoalgaosome size distribution and concentration before and after these treatments (Figure S2c–e). As demonstrated in Figure 3d, the protease treatment of nanoalgaosomes did not impact on esterase activity of protease-treated EV samples; thus, the quantified activity is attributed solely to the esterase within the lumen of the vesicles.

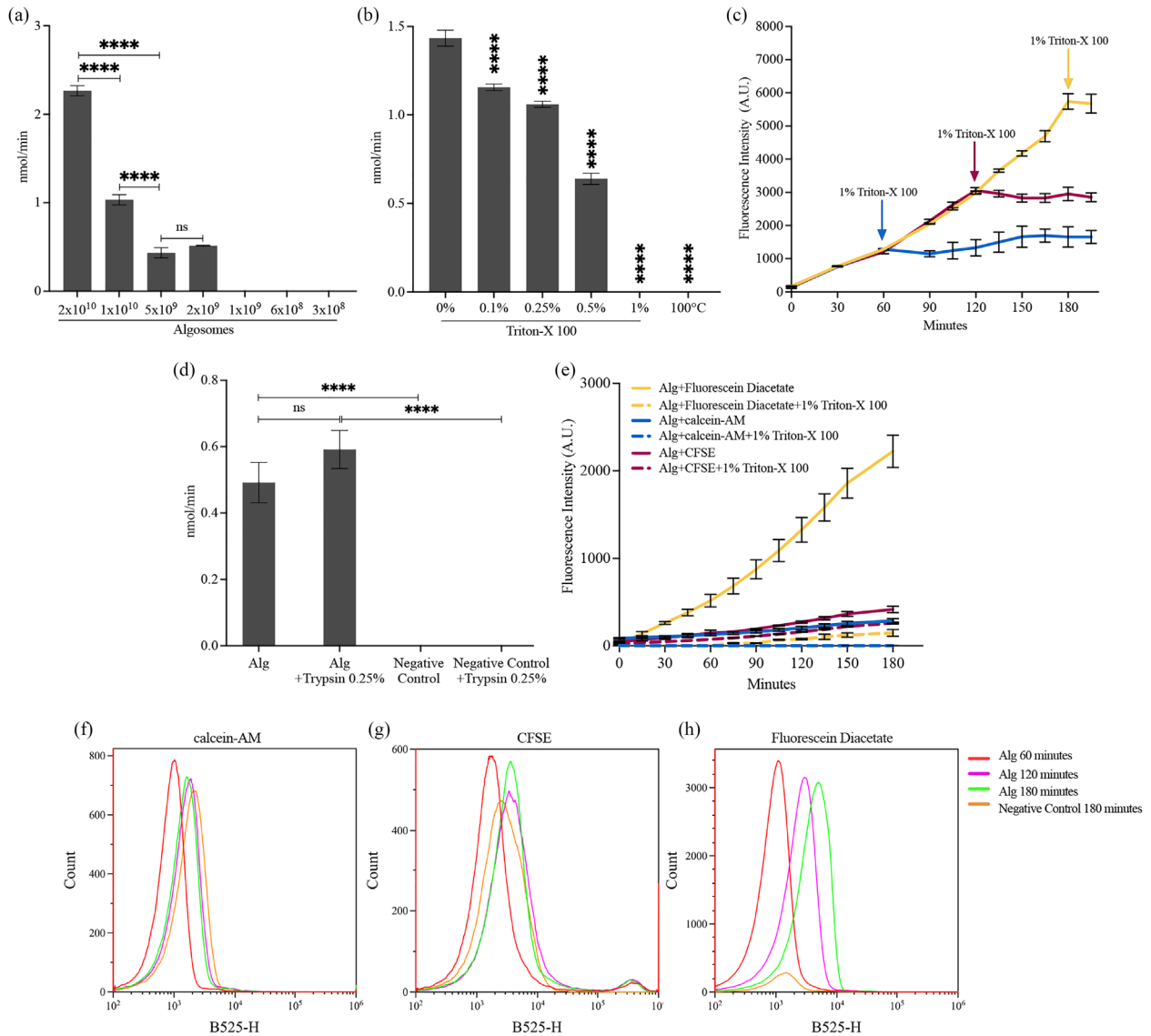


FIGURE 3 Evaluation of the detectEV enzymatic assay sensitivity and specificity, using nanoalgorithms as EV-model. (a) Detection limit determination using different concentrations of nanoalgorithms ranging from 2×10^{10} to 3×10^8 sEVs. Error bars represent the standard deviation of the mean of independent experiments ($n = 3$). One-way ANOVA was used to assess the statistical significance of the differences, showing $****p < 0.0001$ and ns differences. (b) Enzymatic activity comparison of untreated nanoalgorithms with those treated with various concentrations of Triton-X 100 detergent (0.1%, 0.25%, 0.5%, 1%) or boiled at 100°C . Error bars represent the standard deviation of the mean of independent experiments ($n = 3$). One-way ANOVA was used to assess the statistical significance of differences between untreated nanoalgorithms and those treated with Triton-X 100 at 0.1%, 0.25%, 0.5%, 1%, as well as those boiled at 100°C , showing $****p < 0.0001$ for all conditions. (c) Fluorescence intensity measurements of nanoalgorithms treated with 1% Triton-X 100 after 1, 2, and 3 h following the addition of the fluorescein diacetate substrate. Error bars represent the standard deviation of the mean of the fluorescence intensity (subtracted from the respective PBS with or without 1% Triton-X 100 plus fluorescein diacetate background signal) of independent experiments ($n = 3$). (d) Comparison of the enzymatic activity of nanoalgorithms (Alg) and nanoalgorithms treated with 0.25% Trypsin, along with their respective negative controls (PBS without or with Trypsin 0.25%). Error bars represent the SD of the mean from three independent experiments ($n = 3$). One-way ANOVA was used to assess the statistical significance of differences between untreated nanoalgorithms and those treated with Trypsin 0.25%, showing ns differences; the same test was applied to highlight the differences with the respective controls, showing $****p < 0.0001$. (e) Comparative analysis of esterase-sensitive substrates using fluorescence-based plate reader. The graph shows the fluorescence intensity expressed in arbitrary unit, AU (excitation 488 nm, emission 520 nm) up to 180 min for nanoalgorithms treated or not with 1% Triton-X 100 and incubated with calcein-AM, CFSE and fluorescein diacetate. The fluorescence intensity increases over time, indicating enzymatic activity only when the algosomes are incubated with fluorescein diacetate. Whereas for the calcein-AM and CFSE probes, only a slight increase in fluorescence was observed over time, reaching a very low AU even at 180 min. Error bars represent the standard deviation of the mean of the fluorescence intensity subtracted from the respective background signals measured in the corresponding negative controls, which are: PBS plus calcein-AM, CFSE, or fluorescein diacetate, with and without 1% Triton-X 100). Three independent experiments were considered ($n = 3$). (f-h) Comparative analysis of esterase-sensitive substrates using flow cytometry analyses. Histograms of counts versus fluorescence intensity (blue laser 488 nm) of nanoalgorithms incubated 60, 120, and 180 min with (f) calcein-AM, (g) CFSE, (h) fluorescein diacetate. Negative control samples correspond to PBS incubated 180 min with calcein-AM, CFSE, or fluorescein diacetate. ANOVA, analysis of variance; CFSE, carboxyfluorescein diacetate succinimidyl ester; ns, not significant; sEV, small EV; SD, standard deviation.

Based on the results from this section, the optimal conditions for the detectEV assay will involve incubating 2×10^{10} EVs with 18 μmol of FDA in a PBS solution, with a final reaction volume of 200 μL , in a 96-well plate. Enzymatic activity, measured through fluorescence emission (excitation at 488 nm, emission at 520 nm), will be followed using a spectrofluorometer for a duration of 3 h at room temperature. The final readout corresponds to enzymatic units (nmol/min), which will be calculated using a calibration curve of free fluorescein to derive the total nmols produced during the assay. This value will then be divided by the total time (180 min) to obtain the final readout in nmol/min.

2.4 | Comparative analysis of esterase-sensitive substrates using flow cytometry and fluorescence-based microplate reader

We conducted a comprehensive comparison of the performance of FDA with other esterase-sensitive substrates, including CFSE and calcein-AM, and considered the lipophilic dye PKH67 as an esterase-sensitive negative control. This comparison was carried out using both flow cytometry and fluorescence-based microplate reader readings. The rationale behind this analysis was to explore the features of the detectEV assay by comparing it with similar methodologies and esterase-sensitive substrates. The experimental setup mirrored that of the detectEV assay, exploring the specificity using detergent treatment and recording the fluorescence background of each probe in PBS over time. As shown in Figure 3e–h, nanoalgosomes were incubated with these probes at concentrations reported for EV staining, and the samples were analysed both by fluorescence readings using microplate reader and flow cytometry and for 60, 120, and 180 min (Ender et al., 2020; Tertel et al., 2022).

Figure 3e showed the results of the fluorescence intensity measured using a microplate reader over 180 min, maintaining conditions consistent with the detectEV assay. Calcein-AM and CFSE substrates incubated with nanoalgosomes showed a minor increase in fluorescence over time, and this increase was considerably smaller compared to EV-sample incubated with FDA, even using an equal number of 2×10^{10} EVs.

As shown in Figure S3a, the results for PKH67-fluorescence intensity measurements in EV samples remained constant over time, as expected. Furthermore, calcein-AM and CFSE substrates exhibited a high fluorescent signal in the negative control (PBS) due to substrate auto-hydrolysis, resulting in elevated background values over time. This phenomenon decreased their final fluorescent value, as the background had to be subtracted from those of the respective EV sample in the detectEV setting, thereby reducing the assay's sensitivity when using these substrates compared to FDA (in which the background of the negative control showed a low fluorescence intensity after 180 min). Additionally, in detergent-treated EV samples, the CFSE substrate failed to accurately assess membrane integrity, as there was no difference in the fluorescence signal between samples treated with detergent and those not treated with detergent (Figure 3e). Accordingly, the flow cytometry approach showed that the fluorescence intensity increased over time only in EV samples incubated with the FDA substrate (Figure 3h). This increase was consistent with the esterase activity recorded using the detectEV approach, maintaining a low background fluorescence of the FDA in the negative control (PBS) up to 180 min. In contrast, the calcein-AM and CFSE substrates exhibited a slight increase in fluorescence intensity over time in EV samples (Figure 3f–g). However, the high background values of these substrates in the negative control hindered the evaluation of the EV specific enzymatic activity. For PKH67 staining, the fluorescence intensity remained constant over time in EV samples, reflecting its nature as a lipophilic probe that does not require enzymatic activation (Figure S3b).

These findings demonstrate that esterase-activated probes are ineffective in quantifying the esterase activity within EV lumen using flow cytometry. Although FDA produced the most significant increase in fluorescence, obtaining a quantitative measure of enzymatic activity through flow cytometry remains unfeasible when compared to the detectEV assay.

2.5 | detectEV assay to evaluate human EV integrity and functionality

To assess the detectEV assay's applicability to other EVs, we examined its sensitivity, compatibility, and specificity using various EV types, including EVs isolated from human cell line conditioned media. Accordingly, we employed dUC to isolate sEVs from conditioned media of normal and tumoural mammary epithelial cells, and human embryonic kidney cells (1-7 HB2, MDA-MB 231, and HEK 293T cell lines, respectively). As for nanoalgosomes, we first characterised them by evaluating selected MISEV-2023 quality parameters, confirming the right size distribution, morphology and positivity to enriched EV biomarkers (data reported in Figure S1, EV-TRACK ID: EV231004) (Welsh et al., 2024).

Following the biochemical and biophysical characterization of these three types of sEVs, we incubated 2×10^{10} HEK 293T derived sEVs with 18 μmol of FDA, using the same conditions as for the enzymatic activity evaluation of nanoalgosomes. As shown in Figure 4a, we observed a rapid, time-dependent increase in fluorescence intensity in the sEV samples compared to the negative control. The fluorescence increase follows a kinetic trend similar to that described for macroalgal-derived EVs.

Next, we used different concentrations of HEK 293T derived sEVs to determine the LOD by conducting a dose-response test, as previously described for nanoalgosomes. We incubated different concentrations of HEK 293T derived sEVs from the same

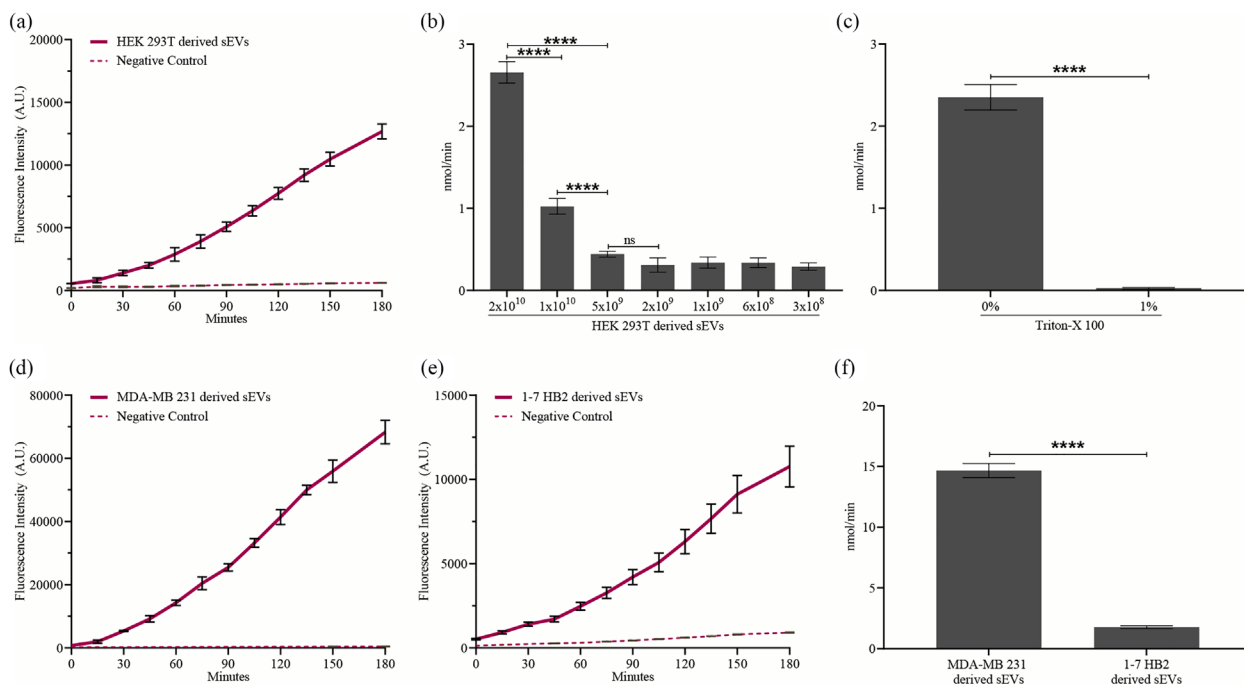


FIGURE 4 DetectEV assay on sEVs derived from different human cell lines. (a) Time-dependent fluorescence increase of HEK 293T sEVs incubated with fluorescein diacetate. Fluorescence intensity (AU, excitation 488 nm, emission 520 nm) of HEK 293T sEVs shows an increase over time, indicating esterase activity and intact vesicles. The PBS control shows minimal fluorescence, confirming signal specificity to vesicle enzymatic activity. (b) Determination of enzymatic activity, expressed in nmol/min, using various concentrations of HEK 293T derived sEVs, ranging from 2×10^{10} to 3×10^8 sEVs. Error bars represent the standard deviation of the mean of independent experiments ($n = 3$). One-way ANOVA was used to assess the statistical significance of the differences, showing **** $p < 0.0001$ and non-significant differences. (c) Enzymatic activity comparison of untreated HEK 293T derived sEVs with those treated with 1% Triton-X 100 detergent, expressed as nmol/min. Error bars represent the standard deviation of the mean of independent experiments ($n = 3$). t -Test was used to assess the statistical significance of differences between untreated nanoalgsomes and those treated with Triton-X 100 at 1%, showing **** $p < 0.0001$. (d–e) Time-dependent fluorescence increase of sEVs isolated from MDA-MB 231 (breast cancer cells), 1–7 HB2 (normal mammary epithelial cells), respectively. sEVs were incubated with fluorescein diacetate, and their fluorescence intensity (AU, excitation at 488 nm, emission at 520 nm) increased over time, indicating esterase activity and the presence of intact vesicles. In contrast, the PBS control exhibited minimal fluorescence, confirming that the signal is specific to the vesicles' enzymatic activity. (f) Enzymatic activity (nmol/min) of sEVs isolated from MDA-MB 231 and 1–7 HB2 cells. Error bars represent the standard deviation of the mean of independent experiments ($n = 3$). t -Test was used to assess the statistical significance of differences between MDA-MB 231 versus 1–7 HB2 derived sEVs, showing **** $p < 0.0001$. ANOVA, analysis of variance; ns, not significant; sEV, small EV.

preparation batch (ranging from 3×10^8 to 2×10^{10} EVs) with FDA. Similar to nanoalgsomes, we found that the enzymatic assay is dose-responsive, with a specific signal up to 1×10^{10} HEK 293T derived sEVs (Figure 4b). We then evaluated the specificity of the detectEV assay using detergent-treated and untreated HEK 293T derived sEVs. The results, shown in the Figure 4c, revealed enzymatic activity of approximately 2.2 nmol/min in 2×10^{10} intact/untreated vesicles, while no activity was detected following 1% Triton-X 100 treatment.

Subsequently, we incubated 2×10^{10} of MDA-MB 231 and 1–7 HB2 derived sEVs with 18 μ mol of FDA, following the detectEV assay setup described earlier. The results in Figure 4d–f confirmed the presence of reliable enzymatic-dependent activity for both of EV types analysed, demonstrating detectEV assay's compatibility with human EVs. Interestingly, breast tumour-derived sEVs showed significantly higher enzymatic activity (5-fold increase) compared to sEVs isolated from normal breast cells, opening new perspectives for detectEV assay's application in tumour diagnosis (Figure 4f).

3 | APPLICATION OF detectEV ASSAY

3.1 | Comparison between EV-isolation methods

Depending on experimental settings and/or the production scale, establishing the most efficient method for EV separation while ensuring sample quality is essential; we previously used various procedures (e.g., dUC and TFF) to efficiently isolate nanoalgsomes from microalgal conditioned media (Adamo et al., 2021; Picciotto et al., 2021). Here, we compared the quality of nanoalgsomes from the same *T. chuii* culture batch, isolated in parallel by dUC and TFF, applying the detectEV assay. The results

indicated that nanoalgosomes isolated by either method showed the same bioactivity/stability, confirming the good quality of both nanoalgosome preparations (Figure 5a).

3.2 | Storage conditions

We applied the detectEV assay to monitor the effects of 1-week storage under different conditions (including 4, -20, -80°C, lyophilization in 5% and 8% sucrose) on nanoalgosome bioactivity/stability (Figure 5b–c). In parallel, we performed NTA readings to monitor the size distribution and concentration of nanoalgosomes stored under these conditions. For all the samples analysed, we did not observe changes in size distribution with an average size of 100 ± 20 nm and a quite similar nanoparticle concentration between the samples (Figures 5c and S4). Conversely, as reported in Figure 5b, the detectEV assay highlighted a significant and quantifiable reduction of enzymatic activity in EV, less than 1 nmol/min in frozen (-20 or -80°C) or lyophilised EV-samples, compared to those stored at 4°C for a week. These results demonstrate that the assay can efficiently identify the most appropriate storage method for EV.

3.3 | Loading methods

EVs are considered a promising novel drug delivery system. To this end, we explored the most reported loading methods for encapsulating biotherapeutics into EVs to determine how external stimuli, such as electrical (i.e., electroporation) or ultrasonic (i.e., sonication) interventions, affect vesicle membrane integrity. This evaluation was conducted without introducing an exogenous cargo, focusing instead on assessing the effectiveness of the proposed assay in detecting changes related to EV integrity. For each method, we used the most commonly reported EV loading settings before applying the detectEV assay (Chen, Sun et al., 2021; Herrmann & Wood, 2021) (Figure 5d). Contextually, we monitored changes in nanoalgosomes size distribution and concentration after the application of each loading method, using NTA (Figure 5e). In Figure 5d, we reported detectEV results, which highlight that freeze and thaw approach appear to be the 'gentlest' loading method, with less impact on nanoalgosome features. In contrast, for some conditions used such as electroporation (E1), sonication (S1), saponification (Sap1-2), or extrusion, we observed a significant decrease in EV-enzymatic activity below 1 nmol/min, probably due to harsh membrane perturbation or loss of vesicle integrity. Interestingly, this difference could not be detected by NTA analysis, as the size (inside the range of 100 ± 20 nm for all samples) and concentration of these samples were similar with the untreated-control (Figure 5e, Figure S5). The successful application of the assay for evaluating EVs during loading could be the starting point for developing effective EV-based therapeutics.

3.4 | Batch-to-batch reproducibility

To assess the detectEV assay's capability in evaluating batch-to-batch reproducibility, we selected four nanoalgosome batches (named Alg1, Alg2, Alg3, Alg4) that exhibited variations in quality during the QC analyses. Following the separation of nanoalgosomes through tangential flow filtration, the application of EV-based QC methods for each production allowed us to identify differences in terms of quality, primarily attributed to the performance or half-life of the TFF cartridges (Adamo et al., 2021; Paolini et al., 2022; Paterna et al., 2022). These differences were revealed by different EV analyses, including fluorescent-NTA readings, after staining 10^{10} nanoalgosomes with di-8-butyl-amino-naphthyl-ethylene-pyridinium-propyl-sulfonate (Di-8-ANEPPS, excitation 488 nm, emission 630 nm), a specific lipophilic fluorescent dye that emit a green fluorescence when it is bound to lipid bilayer. For this reason this dye could help to discriminate between EVs and non-vesicle co-isolates (Adamo et al., 2021). As reported in Figure 5f, the F-NTA results showed that the selected four batches had a quite similar size distribution, but differences in terms of percentage of Di-8-ANEPPS-positive EVs with respect to the total EVs tracked with NTA in scattering. More specifically, Alg1 = 10%; Alg2 = 3%; Alg3 = 2%, Alg4 = unreliable measurement. Subsequently, we applied the detectEV assay for these EV-preparations, using an equal amount of vesicles for all batches (2×10^{10} nanoalgosomes). The results shown in Figure 5g identified Alg1 as the one with high enzymatic activity compared to the other three batches analysed, and are consistent with the F-NTA results (Figure 5f). All these results suggest that the proposed functional enzymatic assay allows for direct and quantitative comparison of EV quality across different isolation methods, storage conditions, and loading conditions. Additionally, it enables the validation of EV preparations and monitoring of batch-to-batch variability during EV production.

3.5 | detectEV prediction of EV functionality

To showcase the predictive capability of the detectEV assay in evaluating the functionality of EVs, we performed an antioxidant activity test as a bioactivity assessment, given the robust antioxidant properties of nanoalgosomes (Adamo et al., 2024). We

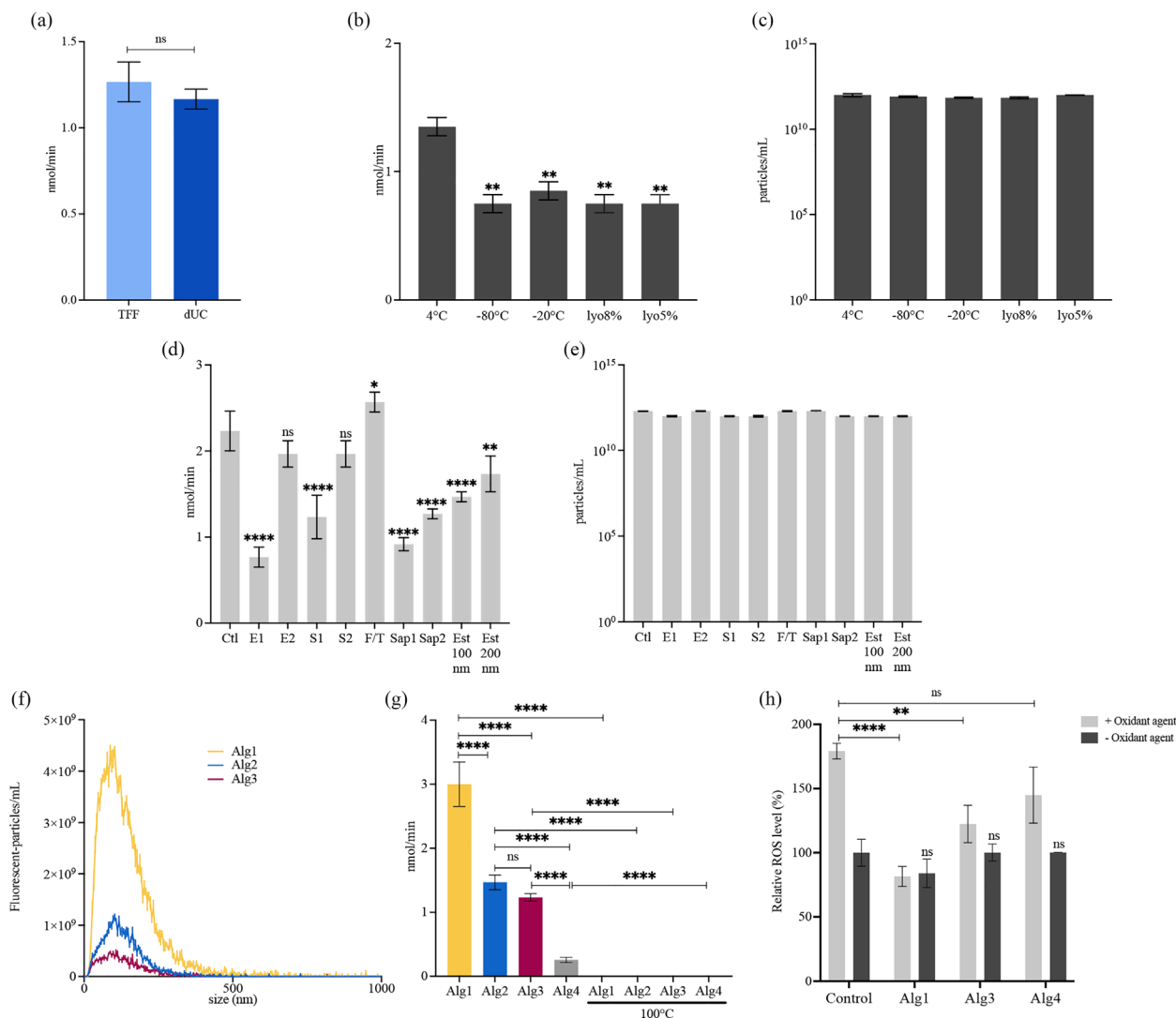


FIGURE 5 DetectEV assay applications. (a) Comparison between nanoalgosomes isolated with different methods. Enzymatic activity (nmol/min) of nanoalgosomes isolated by TFF and dUC. The error bars represent the standard deviation of the mean of independent experiments ($n = 3$). Statistical significance was determined using one-way ANOVA: TFF versus dUC, (b–c) Comparison between nanoalgosomes stored under different conditions. Effect of different storage conditions on nanoalgosomes (i.e., storage for 10 days at 4, –20, –80°C, and lyophilised with 5% and 8% sucrose) analysed by (b) the detectEV assay (nmol/min) and by (c) NTA (particles/mL). In (b) error bars represent the standard deviation of the mean of independent experiments ($n = 3$); in (c) distributions errors are calculated on five replica for each conditions of independent experiments ($n = 3$). One-way ANOVA was used to assess the statistical significance of the differences: 4°C versus –80°C, –20°C, lyo8%, lyo5%; $**p < 0.01$; no significant differences were observed in the NTA data. (d–e) Comparison between nanoalgosomes subjected to various loading methods. Effect of different loading methods on nanoalgosomes analysed by (d) detectEV assay (nmol/min) and (e) NTA (particles/mL). Electroporation settings included E1 (125 μ F, 400 V, 2 pulses of 20 ms) and E2 (125 μ F, 250 V, 2 pulses of 30 ms). Sonication settings included S1 (ultrasonic probe, 20% amplitude, six cycles of 30 s on/off, total 3 min, 2 min cooling, 60 min incubation at 37°C) and S2 (ultrasonic bath, 40 KHz, 40% amplitude, two cycles of 30 s on/off, 60 min incubation at 37°C). F/T consist in three times freeze-thaw cycles at –80°C for 30 min and at RT for 30 min. Saponin treatment included two conditions: Sap1 (0.1 mg/mL) and Sap2 (0.002 mg/mL). Extrusion used polycarbonate membrane filters of 100 nm (Est100nm) and 200 nm (Est200nm) pore size, with each sample extruded 31 times. In (d) error bars represent the standard deviation of the mean of independent experiments ($n = 3$). In (e) distributions errors are calculated on 5 replica of independent experiments ($n = 3$). One-way ANOVA was used to assess statistical significance: Ctl versus (E1, S1, Sap1, Sap2, Est100nm), $****p < 0.0001$; Ctl versus (E2, S2); Ctl versus F/T, $*p < 0.05$; Ctl versus Est200nm, $**p < 0.01$; no significant differences were observed in the NTA data. f–g) Comparison between different nanoalgosome batches. (f) Size distribution of different nanoalgosome batches (Alg1, Alg2, Alg3) stained with a green lyophilic dye (Di-8-ANEPPS), measured by fluorescent-nanoparticle tracking analysis (F-NTA), using NanoSight NS300, with a 500LP filter and a laser wavelength of 488 nm; distributions errors are calculated on five replica of the same batch; F-NTA measurement for Alg4 was unreliable because below the detection limit. (g) detectEV assay on different nanoalgosome batches (Alg1, Alg2, Alg3, Alg4). Error bars represent the standard deviation of the mean of 3 replica of the same batch. One-way ANOVA was used to assess the statistical significance of the differences where indicated, showing non-significant differences; $****p < 0.0001$. (h) Antioxidant activity of different nanoalgosome batches in 1–7 HB2 cells. ROS production in 1–7 HB2 cells treated with 0.5 μ g/mL nanoalgosome for 24 h, with/without oxidant agent (250 μ M TBH), normalised to negative control (untreated cells). Values are presented as means \pm standard deviation from three independent experiments ($n = 3$). Statistical significance of the differences was assessed using one-way ANOVA: 1–7 HB2 (– Oxidant agent) versus 1–7 HB2 treated with Alg1, Alg3, Alg4 (– Oxidant agent); 1–7 HB2 (+ Oxidant agent) versus 1–7 HB2 treated with Alg1 (+ Oxidant agent), $****p < 0.0001$; 1–7 HB2 (+ Oxidant agent) versus 1–7 HB2 treated with Alg3 (+ Oxidant agent), $**p < 0.01$; 1–7 HB2 (+ Oxidant agent) versus 1–7 HB2 treated with Alg4 (+ Oxidant agent). ANOVA, analysis of variance; ns, not significant; dUC, differential ultracentrifugation; TFF, tangential flow filtration.

selected nanoalgosome batches with significant differences in quality, as indicated by the detectEV results showed in Figure 5g. Specifically, we chose Alg1 and Alg3 batches that exhibited significantly higher esterase activity compared to the Alg4 batch.

Subsequently, 1–7 HB2 cells were exposed to 0.5 $\mu\text{g}/\text{mL}$ of Alg1, Alg3, and Alg4 (approximately 10^{10} EVs) to assess their antioxidant bioactivity, particularly in terms of countering reactive oxygen species (ROS) production in cells stressed with the oxidant agent. The results demonstrated that Alg1 and Alg3 effectively mitigated the oxidative stress induced by the oxidant agent, restoring ROS levels near to physiological values, with Alg1 exhibiting strong antioxidant activity (Figure 5h). In contrast, Alg4 failed to alleviate the stress, indicating no significant antioxidant activity. These outcomes align seamlessly with the detectEV results, highlighting its ability to predict the functionality of various EV preparations.

4 | DISCUSSION

The field of EVs has made significant advancements; yet determined challenges persist, primarily centred around the lack of reliable functional assays for assessing EV bioactivity (Nguyen et al., 2020). The intricate nature of EV heterogeneity and their regulated mechanisms across different diseases adds complexity to developing robust and universal functional assays. Despite the diversity of available potency assays, challenges in quantitiveness, sensitivity, accuracy, precision, and robustness persist, emphasizing the urgent need for refining and establishing specific test capable of predicting EV functionality effectively and for different applications (Gimona et al., 2021; Nguyen et al., 2020; Pachler et al., 2017; Ramirez et al., 2018). Also, given the complex nature of EV-based therapeutics, multiple assays are often necessary to capture the various mechanisms of action EV may exhibit, ensuring compliance with regulatory requirements for efficacy and safety. These comprehensive functional evaluations are vital for the successful and safe development of EV-based therapeutic solutions. The bioactivity of EVs can be driven by surface signalling mechanisms, through the transfer of their internal cargo to recipient cells, or a combination of both. In surface signalling, EVs may interact with target cells via receptor-ligand binding or other membrane interactions. On the other hand, cargo transfer refers to the process in which EVs deliver their internal content directly into recipient cells, influencing cellular functions from within.

In this context, this study explores the potential to leverage the presence of active cargo enzymes within EVs for the development of an enzymatic assay to assess the EV integrity. Specifically, our focus has been on esterase-like enzymes in EVs, as their presence is reported in different proteomic datasets, showing associations with EVs from various sources (Choi et al., 2011; Gonzales et al., 2009; Gonzalez-Begne et al., 2009; McMillan & Kuehn, 2022; Pocsfalvi et al., 2018; Rizzo et al., 2020). The proposed detectEV assay specifically aims to quantitatively measure esterase activity within EVs, offering a single-step analysis for assessing the quality of EV preparations, using small-sized samples. Notably, this assay does not require washing steps, making it a faster and cost-effective method that offers several advantages, including simplicity. The establishment of the detectEV assay involved a meticulous validation of specific parameters (e.g., EV and FDA concentrations, reaction volume, reaction buffer, time, and temperature), ensuring analytical sensitivity and specificity, in line with MISEV-2023 guidelines (Welsh et al., 2024). Nanoalgosomes, which are microalgal derived-EVs, were employed as EV models in this validation process. While our results demonstrate that the established experimental settings efficiently measure the enzymatic activity of nanoalgosomes, as well as of EVs derived from different mammalian cell lines, these parameters could be further adapted ad hoc for EVs from various origins or types, like large EVs or oncosomes. Indeed, different types of EVs could exhibit distinct stability or carry different combinations of esterase-like enzymes as cargo, possibly with high enzymatic activity. Consequently, it might be possible to slightly adapt the assay condition, such as by decreasing the amount of FDA, adjusting the reaction time, or vesicle concentration, to establish minimum and maximum ranges of enzymatic activity that qualify vesicle preparations for subsequent analyses. Therefore, the versatile applicability of the detectEV assay across diverse cellular sources allow for its extension to every EV types with esterase-like activity. This positioning makes it a potentially universal measure of EV functionality. The innovation introduced by the detectEV assay is its ability to simultaneously measure both the esterase's enzymatic activity and membrane integrity of vesicles, which is crucial for EV functionality. Specifically, our results illustrated that when the vesicle integrity is perturbed and/or completely lost, the enzymatic activity decrease or becomes undetectable by the detectEV assay. This observation could be attributed to several reasons. First of all, there could be a potential reduction in the enzymatic activity of esterases when released into the extra-vesicular environment, as compared to the optimal condition of the vesicular lumen. The protease treatment of EVs does not affect esterase activities as they are indeed located in the lumen of EVs, demonstrating that detectEV give a measure of bioactive enzymes inside intact vesicles. Moreover, we demonstrated that the detectEV assay extends similar approaches using FDA-like molecules (e.g., calcein-AM or CFSE) already employed to label EVs for flow cytometry analysis (Ender et al., 2020; Kormelink et al., 2016; Nikiforova et al., 2021; Tertel et al., 2022). Our comparative studies showed that using FDA for functional evaluations of EVs outperformed other esterase-sensitive substrates in both flow cytometry and microplate reader analyses, confirming its superiority for assessing the bioactivity of EV luminal cargo and membrane integrity. To note, a precise readout value of EV bioactivity expressed as enzymatic units (nmol/min) is a unique feature that enhances the novelty of the detectEV method, as compared to the fluorescence intensity values (expressed in arbitrary units) provided by calcein-AM or CFSE-based approaches, which allow for a semi-quantitative final value.

Another relevant aspect to consider is the detectEV assay's versatility for different applications. One of these includes monitoring storage conditions of EV preparations. Various studies have demonstrated how different storage conditions can affect EV characteristics, including membrane stability and potency (Jeyaram & Jay, 2017; Sivanantham & Jin, 2022; van de Wakker et al., 2022). Recent comprehensive studies have compared different storage strategies to identify appropriate conditions for stabilizing EV preparations, especially for therapeutic applications (Görgens et al., 2022; Kusuma et al., 2018; Lener et al., 2015; Lőrincz et al., 2014). Following EV sample storage, they are typically analysed using methods like NTA, or flow cytometry (Lőrincz et al., 2014; Sokolova et al., 2011). Our results show that the detectEV assay is more effective than NTA approaches in highlighting slight differences in EV functionality after different storage methods. Numerous studies have highlighted the advantages of using EVs as drug delivery systems in preclinical models due to their low toxicity, high targeting capacity, and slow clearance (Gangadaran & Ahn, 2020). Exogenous cargo can be loaded into EVs using various physical methods, including electroporation, sonication, saponin-assisted loading, freeze-thaw cycles, and extrusion (Fu et al., 2020; Chen, Sun et al., 2021; Van Deun et al., 2020). However, these methods may compromise EV functionality or damage the integrity of their membranes, although the phospholipid bilayer typically restores its integrity quickly after membrane perturbations (Han et al., 2021; Rankin-Turner et al., 2021). In this context, we have demonstrated that the detectEV assay can assess the effects of different loading methods on EVs, highlighting changes or alterations in their luminal bioactivity post-loading; this is because of the assay closely correlates with the bioactivity and quality of the vesicles, as well as the integrity of their membranes. Such capability is crucial for establishing and validating optimal exogenous loading strategies for specific types of EVs, particularly those carrying cargo lacking active components that can react with FDA, thus facilitating their application as nanocarriers for drug delivery in therapeutic contexts (Fu et al., 2020; Lener et al., 2015). Additionally, our findings suggest that the detectEV assay can determine the most effective methods for monitoring specific experimental settings. According to MISEV-2023 guidelines, the quality of EVs can vary significantly based on their source and the scale of production, which necessitates different isolation procedures (Welsh et al., 2024). Our results demonstrate that another valuable application of the detectEV assay is in determining the most suitable isolation methods to monitor specific experimental settings, ensuring the preparation of high-quality bioactive vesicles. Another application described here is its ability to highlight batch-to-batch variation between EV preparations. Indeed, the detectEV results were in complete agreement with the F-NTA data obtained from diverse nanoalgosome batches, showing that higher quality vesicles (Alg1) had also higher enzymatic activity. Additionally, the nanoalgosome batch Alg1 has been shown to be the nanoalgosome preparation that most efficiently counterbalances cell-oxidative stress *in vitro*, as observed in a specific functional test for nanoalgosomes (antioxidant activity assay). This suggests that the detectEV result could predict which vesicle preparation possesses greater specific functionality for subsequent potency test. The assay's future potential to be explored involve developing it as a diagnostic tool to identify pathological signs, such as tumour-derived EVs, based on the evaluation of EV enzymatic activities in liquid biopsy samples (e.g., plasma and urine), aligning with the growing importance of EVs in theranostics (Liang et al., 2021). To conclude, we propose that alongside efforts to harmonise EV nomenclature and characterization, the detectEV assay could represent a solution to existing challenges in functional assays for EVs.

5 | MATERIALS AND METHODS

Nanoalgosomes and cell derived-EVs are isolated and characterised as previously described in Adamo et al. (2021), and the relative methods are reported in Supporting Methods.

5.1 | Set up of functional enzymatic assay: Pilot test

FDA (Sigma-Aldrich) stock solution was prepared in acetone at a final concentration of 2 mg/mL. 2×10^{10} nanoalgosomes were incubated with 35 μ mol of FDA, reaching a final volume of 200 μ L with 0.2 μ m filtered PBS without Ca^{++} and Mg^{++} . The same amount of FDA was added to 0.2 μ m filtered PBS without Ca^{++} and Mg^{++} (nanoalgosome-vehicle). Fluorescence emission was measured every 15 min, up to 16 h, using a blue filter of the GloMax Discover Microplate Reader.

5.2 | Preparation fluorescein standards curve

Fluorescein sodium salt (ex/em 490/514 nm, Sigma-Aldrich) was used to generate a standard calibration curve.

The fluorescence intensity of serial dilutions of fluorescein (from 300 nmol to 0 nmol), diluted in PBS without Ca^{++} and Mg^{++} at a final volume of 200 μ L, was measured in a 96-well-plate using a blue filter of the GloMax Discover Microplate Reader (Promega).

5.3 | Measure of enzymatic activity

To calculate the specific enzymatic activity, the enzyme units (U), the amount of esterases that catalyses the reaction of 1 nmol of substrate into product per minute, was determined. EV enzymatic activity values were expressed in U as nanomoles of fluorescein produced per minute (nmol/min). This value was determined by fitting the fluorescence intensities measured at the end of the functional assay to the fluorescein concentration of the standard curve. Subsequently, this value was divided by the total assay time (180 min) to obtain the nanomoles per minute.

5.4 | Michaelis–Menten Kinetic

2×10^{10} nanoalgosomes were incubated with different concentrations of FDA (0, 1.6, 3.3, 6.6, 13, 26×10^3 nmol) dissolved in 0.2 μm filtered PBS without Ca^{++} and Mg^{++} , in a final volume equal to 200 μL . The fluorescence emission was followed until 3 h, in a 96-well-plate using a blue filter of the GloMax Discover Microplate Reader (Promega). Obtained values were corrected by subtracting background fluorescence value (i.e., PBS with FDA). Fitting these data to the standard calibration curve, the Michaelis–Menten equation was applied using nonlinear regression and plotting the reaction's initial rates (nmol/min) as a function of FDA concentration. V_{max} and K_{m} were found using GraphPad software.

5.5 | Analytical sensitivity

Serial dilutions of nanoalgosomes (from 2×10^{10} to 3×10^8 sEVs) were incubated with 18 μmol of FDA, reaching a final volume of 200 μL with 0.2 μm filtered PBS without Ca^{++} and Mg^{++} . Fluorescence emission was followed up to 3 h, using a blue filter of the GloMax Discover Microplate Reader. The same amount of FDA was added to 0.2 μm -filtered PBS without Ca^{++} and Mg^{++} (nanoalgosome-vehicle). This background fluorescence value was subtracted from the fluorescence intensity values of each sample, for all the condition described. The relative methods of FDA auto-hydrolysis in different media are reported in Supporting Methods.

5.6 | Analytical specificity

2×10^{10} nanoalgosomes were incubated with 0.1, 0.25, 0.5 and 1% Triton-X100 (Sigma-Aldrich) for 30 min at room temperature. The same amount of nanoalgosomes were boiled at 100°C for 10 min. Next, samples were incubated with 18 μmol of FDA, reaching a final volume of 200 μL with 0.2 μm filtered PBS without Ca^{++} and Mg^{++} . Fluorescence emission was followed up to 3 h, and enzymatic activity was determined as described previously. As control, the same amount of FDA was added to 0.2 μm -filtered PBS without Ca^{++} and Mg^{++} boiled at 100°C for 10 min or with 0.1, 0.25, 0.5 and 1% Triton-X 100. This background fluorescence value was subtracted from the fluorescence intensity values of each respective sample.

Additionally, 2×10^{10} nanoalgosomes were incubated with 18 μmol of FDA, reaching a final volume of 200 μL with 0.2 μm filtered PBS without Ca^{++} and Mg^{++} . During the time course of the detectEV assay, specifically after 1, 2, and 3 h post FDA addition, nanoalgosomes were treated with 1% Triton-X 100. Fluorescence emission was measured every 15 min, up to 195 min, using a blue filter of the GloMax Discover Microplate Reader. As control, the same amount of FDA was added to 0.2 μm -filtered PBS with/without Ca^{++} and Mg^{++} with 1% Triton X-100. This background fluorescence value was subtracted from the fluorescence intensity values of each respective sample.

For protease treatment, 10^{11} nanoalgosomes were incubated with a 0.25% (w/v) trypsin solution (Invitrogen, Life Technologies) at 37°C for 15 min. An EV-free control was prepared by using 0.2 μm filtered PBS without Ca^{++} and Mg^{++} . After the digestion period, both EV samples and the negative control underwent a washing step to remove trypsin. Given that FDA can be hydrolysed by proteases, it was essential to eliminate trypsin post-treatment. This was achieved through five washes with PBS using a 100 kDa Amicon filter at low speed ($3000 \times g$ for 5 min, repeated 5 times at 4°C). The absence of trypsin activity was confirmed in the negative control before proceeding with the detectEV assay on the protease-treated EV-samples.

5.7 | Comparative analysis of esterase-sensitive probes

For the comparative study, we used esterase-sensitive probes, including CFSE, calcein acetoxymethyl ester (calcein-AM) (both from Sigma-Aldrich), and the lipophilic dye PKH67 (Sigma-Aldrich) as an esterase-sensitive negative control. Like FDA, calcein-AM is hydrolysed by esterases to produce a polar green-fluorescent product, while CFSE is converted by esterases into an

intermediate that interacts with amines to generate a highly fluorescent green dye. PKH67, a green lipophilic dye, integrates into the membrane without requiring enzymatic activation. Specifically, 2×10^{10} nanoalgsomes were incubated with $10 \mu\text{M}$ calcein-AM, $10 \mu\text{M}$ CFSE (CFDA-SE), and $10 \mu\text{M}$ PKH67, respectively. EV-free PBS solution, used as a negative control, was incubated with the same probes to monitor background signal.

5.8 | Fluorescence-based microplate reader analysis

For the microplate reader analysis, 2×10^{10} nanoalgsomes were incubated with each probe, with and without detergent pretreatment (using 1% Triton X-100 as described before), reaching a final volume of $200 \mu\text{L}$ with $0.2 \mu\text{m}$ filtered PBS without Ca^{++} and Mg^{++} . The same amount of each probe was added at the same concentration to $0.2 \mu\text{m}$ filtered PBS without Ca^{++} and Mg^{++} (used as negative control that correspond to EV-free PBS) with and without 1% Triton X-100. Fluorescence emission was measured every 15 min, up to 3 h, using a blue filter 488 nm on the GloMax Discover Microplate Reader. The background fluorescence value of the negative control was subtracted from the fluorescence intensity values of each respective sample.

5.9 | Flow cytometry

All flow cytometry experiments were performed using a CytoFLEX SRT Cell Sorter (Beckman Coulter), operated with CyExpert SRT software. The CytoFLEX SRT was initialised according to the manufacturer's recommendations to ensure optimal performance. The CytoFLEX SRT used in this study was equipped with three lasers: a red laser (638 nm), a blue laser (488 nm), and a violet laser (405 nm). For the analysis of small particles such as EVs, the configuration was adjusted for violet side scatter (VSSC) detection using the violet (405 nm) laser, and fluorescence detection was performed with the blue laser (488 nm). Megamix-Plus FSC beads (BioCytex), consisting of distinct populations with sizes of 100, 160, 200, 240, 300, 500, and 900 nm, were used to define the size range for EV detection. These beads helped establish the gating strategy for accurately identifying and analysing EVs based on their size. EV samples were diluted 1:20 in $0.2 \mu\text{m}$ filtered PBS without Ca^{++} and Mg^{++} to a final volume of 1 mL. To create a stable and slow-velocity core stream, which is recommended for the detection of EVs, the sample acquisition speed was adjusted. The flow rate was set to $10 \mu\text{L}$ per minute, ensuring precise and consistent sample introduction into the flow cytometer. For each sample, at least 10,000 events were recorded. The acquisition rate was maintained at approximately 6000 events per second to ensure a high-resolution analysis.

5.10 | detectEV assay for human cell-derived sEVs

2×10^{10} sEVs isolated from HEK 293T cells were employed to conduct a time course measurements. After the incubation with $18 \mu\text{mol}$ of FDA, the fluorescence emission was measured every 15 min, up to 180 min, using a blue filter of the GloMax Discover Microplate Reader. As negative control, the same amount of FDA was added to $0.2 \mu\text{m}$ -filtered PBS without Ca^{++} and Mg^{++} . Next, serial dilutions of HEK 293T derived sEVs (from 2×10^{10} to 3×10^8 sEVs) were incubated with $18 \mu\text{mol}$ of FDA, reaching a final volume of $200 \mu\text{L}$ with $0.2 \mu\text{m}$ filtered PBS without Ca^{++} and Mg^{++} . Fluorescence emission was followed up to 3 h, using a blue filter of the GloMax Discover Microplate Reader. The same amount of FDA was added to $0.2 \mu\text{m}$ -filtered PBS without Ca^{++} and Mg^{++} (sEV-vehicle). This background fluorescence value was subtracted from the fluorescence intensity values of each sample, for all the condition described. Further, 2×10^{10} HEK 293T derived sEVs were incubated with 1% Triton-X 100 for 30 min at room temperature. Next, EV-samples were incubated with $18 \mu\text{mol}$ of FDA, reaching a final volume of $200 \mu\text{L}$ with $0.2 \mu\text{m}$ filtered PBS without Ca^{++} and Mg^{++} . Fluorescence emission was followed up to 3 h, and enzymatic activity was determined as described previously. As control, the same amount of FDA was added to $0.2 \mu\text{m}$ -filtered PBS without Ca^{++} and Mg^{++} with 1% Triton-X 100. This background fluorescence value was subtracted from the fluorescence intensity values of each respective sample. For MDA-MB231 and 1-7 HB2 cell derived EVs, 2×10^{10} sEVs were employed to conduct the detectEV assay, using the same experimental setting described before.

6 | APPLICATION OF detectEV ASSAY

6.1 | Isolation methods

2×10^{10} nanoalgsomes of the same *T. chuii* conditioned media, isolated by dUC and TFF, were used to perform the functional enzymatic assay, using the same settings described before (Adamo et al., 2021). A detailed description of methods used for EV isolation are reported in Supporting Methods.

6.2 | Storage conditions

Nanoalgosomes were stored for 10 days at different condition: 4, -20 , -80°C and upon lyophilization in 5% and 8% sucrose, at 4°C for a week. Lyophilised samples were carefully rehydrated in $0.2\ \mu\text{m}$ -filtered Milli-Q water. After NTA analysis on all stored samples, detectEV assay was performed, as described previously.

6.3 | Loading methods

2×10^{12} nanoalgosomes (and nanoalgosome-vehicle, i.e., $0.2\ \mu\text{m}$ filtered PBS without Ca^{++} and Mg^{++} , used as a negative control) underwent the subsequent treatments

- Electroporation was performed in Gene Pulser cuvettes ($0.4\ \text{cm}$ cell electrode gap) on a BioRad Gene Pulser equipped with a capacitance extender, with two conditions selected, E1 ($125\ \mu\text{F}$, $400\ \text{V}$ and 2 pulse time of 20 ms) and E2 ($125\ \mu\text{F}$, $250\ \text{V}$ and 2 pulse time of 30 ms).
- Sonication was performed using two settings: ultrasonic probe sonicator (S1) with 20% amplitude for six cycles of 30 s on/off for a total of 3 min, with 2 min cooling, then incubation for 60 min at 37°C ; ultrasonic bath (S2) 40 KHz, 40% amplitude for 2 cycles of 30 s on/off, then incubation for 60 min at 37°C .
- Freeze–Thaw was performed in 3 cycles of freezing at -80° for 30 min and thawing at room temperature (RT) for 30 min.
- Saponin treatment was performed using two settings: incubation with $0.1\ \text{mg/mL}$ (Sap1) and $0.002\ \text{mg/mL}$ (Sap2) of saponin (Sigma-Aldrich) at RT for 10 min.
- Extrusion using a mini-extruder equipped with polycarbonate membrane filters of $100\ \text{nm}$ and $200\ \text{nm}$ pore size (Avestin, Mannheim, Germany). Each sample was extruded 31 times.

After the application of each method, NTA analysis was performed on all samples. Next, the enzymatic functional assay was performed, as described previously.

6.4 | Batch-to-batch reproducibility

2×10^{10} nanoalgosomes from different batches (named Alg1, Alg2, Alg3, and Alg4) were incubated with $18\ \mu\text{mol}$ of FDA, reaching a final volume of $200\ \mu\text{L}$ with $0.2\ \mu\text{m}$ filtered PBS without Ca^{++} and Mg^{++} . Fluorescence emission was followed up to 3 h, and enzymatic activity was determined as described above. As negative controls, nanoalgosomes were boiled at 100°C for 10 min.

6.5 | Antioxidant activity assay

Intracellular ROS levels in living cells were assessed by employing 2', 7'-dichlorofluorescein diacetate (DCF-DA; Sigma-Aldrich). DCF-DA undergoes oxidation to form fluorescent DCF (2', 7'-dichlorofluorescein) in the presence of ROS, enabling detection using a spectrofluorometer. The antioxidant assay was conducted on 1–7 HB2 cell line. Specifically, 4×10^3 cells were plated in 96-well microplates for 24 h. Subsequently, cells were treated with Alg1, Alg3, and Alg4 ($0.5\ \mu\text{g/mL}$, 10^{10} EVs/mL) for an additional 24 h. Following removal of the medium, cells were exposed to PBS containing $40\ \mu\text{M}$ of DCF-DA and incubated in a humidified atmosphere ($5\% \text{CO}_2$ at 37°C) for 1 h. The cells were then subjected to treatment with or without the oxidative agents TBH ($250\ \mu\text{M}$ for 1 h) (tert-butyl hydroperoxide solution, Sigma-Aldrich), in the absence or presence of nanoalgosomes. Untreated cells served as a control to establish the baseline intracellular ROS percentage. After thorough washing steps, fluorescence intensity was measured using a fluorescence plate reader with an excitation wavelength of $485\ \text{nm}$ and an emission wavelength of $538\ \text{nm}$ (GloMax® Discover Microplate Reader, Promega). The relative percentage of intracellular ROS was normalised respect to untreated cells (control).

6.6 | Statistical analysis

GraphPad Prism version 10 was used for statistical analysis. *t*-Test, one-way analysis of variance (ANOVA) or Two-way analysis of variance (ANOVA) followed by Tukey's multiple comparisons were performed when two, three or more than three means of independent groups were compared, respectively. Statistical significance was set as $p < 0.05$ and star significance were distributed as * for $p < 0.05$, ** for $p < 0.01$, *** for $p < 0.001$, and **** for $p < 0.0001$, while ns correspond to non-significant differences. Each measurement reported here was repeated as experimental triplicate, and mean values, as well as standard deviations, were calculated.

AUTHOR CONTRIBUTIONS

Giorgia Adamo: Conceptualization (lead); data curation (lead); formal analysis (lead); funding acquisition (supporting); investigation (lead); methodology (lead); project administration (supporting); supervision (lead); validation (lead); visualization (lead); writing – original draft (lead); writing – review and editing (lead). **Sabrina Picciotto:** Data curation (lead); formal analysis (lead); investigation (equal); methodology (lead); software (equal); validation (equal); writing – original draft (lead); writing – review and editing (lead). **Paola Gargano:** Data curation (equal); formal analysis (equal); software (equal); writing – original draft (equal). **Angela Paterna:** Data curation (supporting); formal analysis (supporting). **Samuele Raccosta:** Data curation (supporting); formal analysis (supporting). **Estella Rao:** Data curation (supporting); formal analysis (supporting). **Daniele Paolo Romancino:** Data curation (equal); formal analysis (equal). **Giulio Gherzi:** Data curation (equal); formal analysis (equal). **Mauro Manno:** Data curation (equal); formal analysis (equal); writing – original draft (equal). **Monica Salamone:** Data curation (equal); formal analysis (equal). **Antonella Bongiovanni:** Conceptualization (lead); funding acquisition (lead); investigation (lead); project administration (lead); resources (lead); validation (lead); visualization (lead); writing – original draft (lead); writing – review and editing (lead).

ACKNOWLEDGEMENTS

This work was supported by the VES4US and the BOW projects, funded by the European Union's Horizon 2020 research and innovation programme, under grant agreements nos. 801338 and 952183, MUR PNRR 'National Center for Gene Therapy and Drugs based on RNA Technology' (Project no. CN00000041 CN3 RNA) and by the Institute for Research and Biomedical Innovation (IRIB), National Research Council of Italy (CNR) of Palermo (Internal Call@IRIB2023).

CONFLICT OF INTEREST STATEMENT

The authors declare the following financial competing interests: A.B., M.M., and N.T. have filed the patent (PCT/EP2020/086622) related to microalgal-derived extracellular vesicles described in the paper. A.B., M.M., and N.T. are co-founders and A.B. CEO of EVEBiofactory s.r.l. G.A., S.P., and A.B. have filed the patent (PCT/IB2024/052194) related to the detectEV assay. The remaining authors declare no competing interests.

ORCID

Giorgia Adamo  <https://orcid.org/0000-0002-6887-763X>

REFERENCES

- Adam, G., & Duncan, H. (2001). Development of a sensitive and rapid method for the measurement of total microbial activity using fluorescein diacetate (FDA) in a range of soils. *Soil Biology and Biochemistry*, 33, 943–951.
- Adamo, G., Fierli, D., Romancino, D. P., Picciotto, S., Barone, M. E., Aranyos, A., Božič, D., Morsbach, S., Raccosta, S., Stanly, C., Paganini, C., Gai, M., Cusimano, A., Martorana, V., Noto, R., Carrotta, R., Librizzi, F., Randazzo, L., Parkes, R., ... Bongiovanni, A. (2021). Nanoalgosomes: Introducing extracellular vesicles produced by microalgae. *Journal of Extracellular Vesicles*, 10(6), e12081. <https://doi.org/10.1002/jev2.12081>
- Adamo, G., Santonicola, P., Picciotto, S., Gargano, P., Nicosia, A., Longo, V., Aloï, N., Romancino, D. P., Paterna, A., Rao, E., Raccosta, S., Noto, R., Salamone, M., Deidda, I., Costa, S., Di Sano, C., Zampi, G., Morsbach, S., Landfester, K., ... Bongiovanni, A. (2024). Extracellular vesicles from the microalga *Tetraselmis chuii* are biocompatible and exhibit unique bone tropism along with antioxidant and anti-inflammatory properties. *Communications Biology*, 7(1), 941. <https://doi.org/10.1038/s42003-024-06612-9>
- Bisswanger, H. (2014). Enzyme assays. *Perspectives in Science*, 1, 41–55.
- Bleackley, M. R., Samuel, M., Garcia-Ceron, D., McKenna, J. A., Lowe, R. G. T., Pathan, M., Zhao, K., Ang, C. S., Mathivanan, S., & Anderson, M. A. (2020). Extracellular vesicles from the cotton pathogen *Fusarium oxysporum* f. sp. *vasinfectum* induce a phytotoxic response in plants. *Frontiers in Plant Science*, 10, 1610. <https://doi.org/10.3389/fpls.2019.01610>
- Chen, C., Sun, M., Wang, J., Su, L., Lin, J., & Yan, X. (2021). Active cargo loading into extracellular vesicles: Highlights the heterogeneous encapsulation behaviour. *Journal of Extracellular Vesicles*, 10(13), e12163. <https://doi.org/10.1002/jev2.12163>
- Chen, Y., Zhao, Y., Yin, Y., Jia, X., & Mao, L. (2021). Mechanism of cargo sorting into small extracellular vesicles. *Bioengineered*, 12(1), 8186–8201. <https://doi.org/10.1080/21655979.2021.1977767>
- Choi, B., Rempala, G. A., & Kim, J. K. (2017). Beyond the Michaelis-Menten equation: Accurate and efficient estimation of enzyme kinetic parameters. *Scientific Reports*, 7(1), 17018. <https://doi.org/10.1038/s41598-017-17072-z>
- Choi, D. S., Kim, D. K., Choi, S. J., Lee, J., Choi, J. P., Rho, S., Park, S. H., Kim, Y. K., Hwang, D., & Gho, Y. S. (2011). Proteomic analysis of outer membrane vesicles derived from *Pseudomonas aeruginosa*. *Proteomics*, 11(16), 3424–3429. <https://doi.org/10.1002/pmic.201000212>
- Cyglér, M., Schrag, J. D., Sussman, J. L., Harel, M., Silman, I., Gentry, M. K., & Doctor, B. P. (1993). Relationship between sequence conservation and three-dimensional structure in a large family of esterases, lipases, and related proteins. *Protein Science*, 2(3), 366–382. <https://doi.org/10.1002/pro.5560020309>
- de Rond, L., van der Pol, E., Hau, C. M., Varga, Z., Sturk, A., van Leeuwen, T. G., Nieuwland, R., & Coumans, F. A. W. (2018). Comparison of generic fluorescent markers for detection of extracellular vesicles by flow cytometry. *Clinical Chemistry*, 64(4), 680–689. <https://doi.org/10.1373/clinchem.2017.278978>
- Duggleby, R. G. (1979). Experimental designs for estimating the kinetic parameters for enzyme-catalysed reactions. *Journal of Theoretical Biology*, 81(4), 671–684. [https://doi.org/10.1016/0022-5193\(79\)90276-5](https://doi.org/10.1016/0022-5193(79)90276-5)
- Duggleby, R. G., & Wood, C. (1989). Analysis of progress curves for enzyme-catalysed reactions. Automatic construction of computer programs for fitting integrated rate equations. *The Biochemical Journal*, 258(2), 397–402. <https://doi.org/10.1042/bj2580397>
- Dzionek, A., Dzik, J. M., Wojcieszynska, D., & Guzik, U. (2018). Fluorescein diacetate hydrolysis using the whole biofilm as a sensitive tool to evaluate the physiological state of immobilized bacterial cells. *Catalysts*, 8, 434.

- Ender, F., Zamzow, P., Bubnoff, N. V., & Gieseler, F. (2020). Detection and quantification of extracellular vesicles via FACS: Membrane labeling matters! *International Journal of Molecular Sciences*, 21(1), 291. <https://doi.org/10.3390/ijms21010291>
- Fontvieille, D. A., Outaguerouine, A., & Thevenot, D. R. (1992). Fluorescein diacetate hydrolysis as a measure of microbial activity in aquatic systems: Application to activated sludges. *Environmental Technology*, 13, 531–540.
- Fu, S., Wang, Y., Xia, X., & Zheng, J. C. (2020). Exosome engineering: Current progress in cargo loading and targeted delivery. *NanoImpact*, 20, 100261.
- Gangadaran, P., & Ahn, B.-C. (2020). Extracellular vesicle- and extracellular vesicle mimetics-based drug delivery systems: New perspectives, challenges, and clinical developments. *Pharmaceutics*, 12, 442.
- Garcia-Ceron, D., Lowe, R. G. T., McKenna, J. A., Brain, L. M., Dawson, C. S., Clark, B., Berkowitz, O., Faou, P., Whelan, J., Bleackley, M. R., & Anderson, M. A. (2021). Extracellular vesicles from *Fusarium graminearum* contain protein effectors expressed during infection of corn. *Journal of Fungi*, 7(11), 977. <https://doi.org/10.3390/jof7110977>
- Gimona, M., Brizzi, M. F., Choo, A. B. H., Dominici, M., Davidson, S. M., Grillari, J., Hermann, D. M., Hill, A. F., de Kleijn, D., Lai, R. C., Lai, C. P., Lim, R., Monguió-Tortajada, M., Muraca, M., Ochiya, T., Ortiz, L. A., Toh, W. S., Yi, Y. W., Witwer, K. W., ... Lim, S. K. (2021). Critical considerations for the development of potency tests for therapeutic applications of mesenchymal stromal cell-derived small extracellular vesicles. *Cytotherapy*, 23(5), 373–380. <https://doi.org/10.1016/j.jcyt.2021.01.001>
- Gonzales, P. A., Pisitkun, T., Hoffert, J. D., Tchapyjnikov, D., Star, R. A., Kleta, R., Wang, N. S., & Knepper, M. A. (2009). Large-scale proteomics and phosphoproteomics of urinary exosomes. *Journal of the American Society of Nephrology*, 20(2), 363–379. <https://doi.org/10.1681/ASN.2008040406>
- Gonzalez-Begne, M., Lu, B., Han, X., Hagen, F. K., Hand, A. R., Melvin, J. E., & Yates, J. R. (2009). Proteomic analysis of human parotid gland exosomes by multidimensional protein identification technology (MudPIT). *Journal of Proteome Research*, 8(3), 1304–1314. <https://doi.org/10.1021/pr800658c>
- Görgens, A., Corso, G., Hagey, D. W., Wiklander, J., Gustafsson, M. O., Felldin, U., Lee, Y., Bostancioglu, R. B., Sork, H., Liang, X., Zheng, W., Mohammad, D. K., van de Wakker, S. I., Vader, P., Zickler, A. M., Mamand, D. R., Ma, L., Holme, M. N., Stevens, M. M., ... El Andaloussi, S. (2022). Identification of storage conditions stabilizing extracellular vesicles preparations. *Journal of Extracellular Vesicles*, 11(6), e12238. <https://doi.org/10.1002/jev2.12238>
- Gray, W. D., Mitchell, A. J., & Searles, C. D. (2015). An accurate, precise method for general labeling of extracellular vesicles. *MethodsX*, 2, 360–367.
- Han, Y., Jones, T. W., Dutta, S., Zhu, Y., Wang, X., Narayanan, S. P., Fagan, S. C., & Zhang, D. (2021). Overview and update on methods for cargo loading into extracellular vesicles. *Processes*, 9(2), 356. <https://doi.org/10.3390/pr9020356>
- Herrmann, I. K., Wood, M. J. A., & Fuhrmann, G. (2021). Extracellular vesicles as a next-generation drug delivery platform. *Nature Nanotechnology*, 16, 748–759.
- Hutter, J. L., & Bechhoefer, J. (1993). Calibration of atomic-force microscope tips. *Review of Scientific Instruments*, 64, 1868–1873.
- Jamur, M. C., & Oliver, C. (2010). Permeabilization of cell membranes. *Methods in Molecular Biology*, 588, 63–66.
- Jeyaram, A., & Jay, S. M. (2017). Preservation and storage stability of extracellular vesicles for therapeutic applications. *The AAPS Journal*, 20(1), 1.
- Kormelink, T. G., Arkesteijn, G. J. A., Nauwelaers, F. A., & van den Engh, G., Nolte-^t Hoen, E. N. M., Wauben, M. H. M. (2016). Prerequisites for the analysis and sorting of extracellular vesicle subpopulations by high-resolution flow cytometry. *Cytometry Part A*, 89, 135–147.
- Kusuma, G. D., Barabadi, M., Tan, J. L., Morton, D. A. V., Frith, J. E., & Lim, R. (2018). To protect and to preserve: Novel preservation strategies for extracellular vesicles. *Frontiers in Pharmacology*, 9, 1199.
- LeClaire, M., Gimzewski, J., & Sharma, S. (2021). A review of the biomechanical properties of single extracellular vesicles. *Nano Select*, 2, 1–15.
- Lener, T., Gimona, M., Aigner, L., Börger, V., Buzas, E., Camussi, G., Chaput, N., Chatterjee, D., Court, F. A., Del Portillo, H. A., O'Driscoll, L., Fais, S., Falcon-Perez, J. M., Felderhoff-Mueser, U., Fraile, L., Gho, Y. S., Görgens, A., Gupta, R. C., Hendrix, A., ... Giebel, B. (2015). Applying extracellular vesicles based therapeutics in clinical trials—An ISEV position paper. *Journal of Extracellular Vesicles*, 4, 30087. <https://doi.org/10.3402/jev.v4.30087>
- Liang, Y., Lehrich, B. M., Zheng, S., & Lu, M. (2021). Emerging methods in biomarker identification for extracellular vesicle-based liquid biopsy. *Journal of Extracellular Vesicles*, 10, e12090.
- Lórinz, Á. M., Timár, C. I., Marosvári, K. A., Veres, D. S., Otrókoci, L., Kittel, Á., & Ligeti, E. (2014). Effect of storage on physical and functional properties of extracellular vesicles derived from neutrophilic granulocytes. *Journal of Extracellular Vesicles*, 3, 25465. <https://doi.org/10.3402/jev.v3.25465>
- McMillan, H. M., & Kuehn, M. J. (2022). Proteomic profiling reveals distinct bacterial extracellular vesicle subpopulations with possibly unique functionality. *Applied and Environmental Microbiology*, 89, e01686–e01622.
- Michaelis, L., Menten, M. L., Johnson, K. A., & Goody, R. S. (2011). The original Michaelis constant: Translation of the 1913 Michaelis-Menten paper. *Biochemistry*, 50, 8264–8269.
- Morales-Kastresana, A., Telford, B., Musich, T. A., McKinnon, K., Clayborne, C., Braig, Z., Rosner, A., Demberg, T., Watson, D. C., Karpova, T. S., Freeman, G. J., DeKruyff, R. H., Pavlakis, G. N., Terabe, M., Robert-Guroff, M., Berzofsky, J. A., & Jones, J. C. (2017). Labeling extracellular vesicles for nanoscale flow cytometry. *Scientific Reports*, 7(1), 1878. <https://doi.org/10.1038/s41598-017-01731-2>
- Nguyen, V. V. T., Witwer, K. W., Verhaar, M. C., Strunk, D., & van Balkom, B. W. M. (2020). Functional assays to assess the therapeutic potential of extracellular vesicles. *Journal of Extracellular Vesicles*, 10, e12033.
- Nikiforova, N., Chumachenko, M., Nazarova, I., Zabegina, L., Slyusarenko, M., Sidina, E., & Malek, A. (2021). CM-Dil staining and SEC of plasma as an approach to increase sensitivity of extracellular nanovesicles quantification by bead-assisted flow cytometry. *Membranes*, 11(7), 526. <https://doi.org/10.3390/membranes11070526>
- O'Grady, T., Njock, M. S., Lion, M., Bruyr, J., Mariavelle, E., Galvan, B., Boeckx, A., Struman, I., & Dequiedt, F. (2022). Sorting and packaging of RNA into extracellular vesicles shape intracellular transcript levels. *BMC Biology*, 20(1), 72. <https://doi.org/10.1186/s12915-022-01277-4>
- Pachler, K., Ketterl, N., Desgeorges, A., Dunai, Z. A., Laner-Plamberger, S., Streif, D., Strunk, D., Rohde, E., & Gimona, M. (2017). An in vitro potency assay for monitoring the immunomodulatory potential of stromal cell-derived extracellular vesicles. *International Journal of Molecular Sciences*, 18(7), 1413. <https://doi.org/10.3390/ijms18071413>
- Paolini, L., Monguió-Tortajada, M., Costa, M., Antenucci, F., Barilani, M., Clos-Sansalvador, M., Andrade, A. C., Driedonks, T. A. P., Giancaterino, S., Kronstadt, S. M., Mizenko, R. R., Nawaz, M., Osteikoetxea, X., Pereira, C., Shrivastava, S., Boysen, A. T., van de Wakker, S. I., van Herwijnen, M. J. C., Wang, X., ... Bergese, P. (2022). Large-scale production of extracellular vesicles: Report on the "massivEVs" ISEV workshop. *Journal of Extracellular Biology*, 1(10), e63. <https://doi.org/10.1002/jex2.63>
- Paterna, A., Rao, E., Adamo, G., Raccosta, S., Picciotto, S., Romancino, D., Noto, R., Touzet, N., Bongiovanni, A., & Manno, M. (2022). Isolation of extracellular vesicles from microalgae: A renewable and scalable bioprocess. *Frontiers in Bioengineering and Biotechnology*, 10, 836747. <https://doi.org/10.3389/fbioe.2022.836747>
- Perna, R. F., Tiosso, P. C., Sgobi, L. M., Vieira, A. M. S., Vieira, M. F., Tardioli, P. W., Soares, C. M. F., & Zanin, G. M. (2017). Effects of Triton X-100 and PEG on the catalytic properties and thermal stability of lipase from *Candida Rugosa* free and immobilized on glyoxyl-agarose. *The Open Biochemistry Journal*, 11, 66–76. <https://doi.org/10.2174/1874091X01711010066>

- Picciotto, S., Barone, M. E., Fierli, D., Aranyos, A., Adamo, G., Božič, D., Romancino, D. P., Stanly, C., Parkes, R., Morsbach, S., Raccosta, S., Paganini, C., Cusimano, A., Martorana, V., Noto, R., Carrotta, R., Librizzi, F., Capasso Palmiero, U., Santonicola, P., ... Bongiovanni, A. (2021). Isolation of extracellular vesicles from microalgae: Towards the production of sustainable and natural nanocarriers of bioactive compounds. *Biomaterials Science*, 9(8), 2917–2930. <https://doi.org/10.1039/d0bm01696a>
- Picciotto, S., Santonicola, P., Paterna, A., Rao, E., Raccosta, S., Romancino, D. P., Noto, R., Touzet, N., Manno, M., Di Schiavi, E., Bongiovanni, A., & Adamo, G. (2022). Extracellular vesicles from microalgae: Uptake studies in human cells and *Caenorhabditis elegans*. *Frontiers in Bioengineering and Biotechnology*, 10, 830189. <https://doi.org/10.3389/fbioe.2022.830189>
- Pocsfalvi, G., Turiák, L., Ambrosone, A., Del Gaudio, P., Puska, G., Fiume, I., Silvestre, T., & Vékey, K. (2018). Protein biocargo of citrus fruit-derived vesicles reveals heterogeneous transport and extracellular vesicle populations. *Journal of Plant Physiology*, 229, 111–121. <https://doi.org/10.1016/j.jplph.2018.07.006>
- Pospichalova, V., Svoboda, J., Dave, Z., Kotrbova, A., Kaiser, K., Klemova, D., Ilkovic, L., Hampl, A., Crha, I., Jandakova, E., Minar, L., Weinberger, V., & Bryja, V. (2015). Simplified protocol for flow cytometry analysis of fluorescently labeled exosomes and microvesicles using dedicated flow cytometer. *Journal of Extracellular Vesicles*, 4, 25530. <https://doi.org/10.3402/jev.v4.25530>
- Ramirez, M. I., Amorim, M. G., Gadelha, C., Milic, I., Welsh, J. A., Freitas, V. M., Nawaz, M., Akbar, N., Couch, Y., Makin, L., Cooke, F., Vettore, A. L., Batista, P. X., Freezor, R., Pezuk, J. A., Rosa-Fernandes, L., Carreira, A. C. O., Devitt, A., Jacobs, L., ... Dias-Neto, E. (2018). Technical challenges of working with extracellular vesicles. *Nanoscale*, 10(3), 881–906. <https://doi.org/10.1039/c7nr08360b>
- Rankin-Turner, S., Vader, P., O'Driscoll, L., Giebel, B., Heaney, L. M., & Davies, O. G. (2021). A call for the standardised reporting of factors affecting the exogenous loading of extracellular vesicles with therapeutic cargos. *Advanced Drug Delivery Reviews*, 173, 479–491.
- Raposo, G., & Stoorvogel, W. (2013). Extracellular vesicles: Exosomes, microvesicles, and friends. *Journal of Cell Biology*, 200(4), 373–383.
- Rizzo, J., Chaze, T., Miranda, K., Roberson, R. W., Gorgette, O., Nimrichter, L., Matondo, M., Latgé, J. P., Beauvais, A., & Rodrigues, M. L. (2020). Characterization of extracellular vesicles produced by *Aspergillus fumigatus* protoplasts. *mSphere*, 5(4), e00476–e00420. <https://doi.org/10.1128/mSphere.00476-20>
- Robinson, P. K. (2015). Enzymes: Principles and biotechnological applications. *Essays in Biochemistry*, 59, 1–41.
- Russell, A. E., Sneider, A., Witwer, K. W., Bergese, P., Bhattacharyya, S. N., Cocks, A., Cocucci, E., Erdbrügger, U., Falcon-Perez, J. M., Freeman, D. W., Gallagher, T. M., Hu, S., Huang, Y., Jay, S. M., Kano, S. I., Lavieu, G., Leszczynska, A., Llorente, A. M., Lu, Q., ... Vader, P. (2019). Biological membranes in EV biogenesis, stability, uptake, and cargo transfer: An ISEV position paper arising from the ISEV membranes and EVs workshop. *Journal of Extracellular Vesicles*, 8(1), 1684862. <https://doi.org/10.1080/20013078.2019.1684862>
- Simpson, R. J., & Kalra, H., & Mathivanan, S. (2012). ExoCarta as a resource for exosomal research. *Journal of Extracellular Vesicles*, 1, 18374.
- Sirt Çıplak, E., & Akoğlu, K. G. (2020). Enzymatic activity as a measure of total microbial activity on historical stone. *Heritage*, 3, 671–681.
- Sivanantham, A., & Jin, Y. (2022). Impact of storage conditions on EV integrity/surface markers and cargos. *Life*, 12, 697.
- Sokolova, V., Ludwig, A. K., Hornung, S., Rotan, O., Horn, P. A., Epple, M., & Giebel, B. (2011). Characterisation of exosomes derived from human cells by nanoparticle tracking analysis and scanning electron microscopy. *Colloids and Surfaces. B, Biointerfaces*, 87(1), 146–150. <https://doi.org/10.1016/j.colsurfb.2011.05.013>
- Sun, Y., Liu, G., Zhang, K., Cao, Q., Liu, T., & Li, J. (2021). Mesenchymal stem cells-derived exosomes for drug delivery. *Stem Cell Research & Therapy*, 12, 561.
- Sverdlöv, E. D. (2012). Amedeo Avogadro's cry: What is 1 µg of exosomes? *BioEssays*, 34, 873–875.
- Tertel, T., Schoppet, M., Stambouli, O., Al-Jipouri, A., James, P. F., & Giebel, B. (2022). Imaging flow cytometry challenges the usefulness of classically used extracellular vesicle labeling dyes and qualifies the novel dye Exoria for the labeling of mesenchymal stromal cell–extracellular vesicle preparations. *Cytotherapy*, 24, 619–628.
- USA FDA—Guidance for Industry Potency Tests for Cellular and Gene Therapy Products. (2011). <https://www.fda.gov/files/vaccines,%20blood%20%26%20biologics/published/Final-Guidance-for-Industry-Potency-Tests-for-Cellular-and-Gene-Therapy-Products.pdf>
- EV-TRACK Consortium. Van Deun, J., Mestdagh, P., Agostinis, P., Akay, Ö., Anand, S., Anckaert, J., Martinez, Z. A., Baetens, T., Beghein, E., Bertier, L., Berx, G., Boere, J., Boukouris, S., Bremer, M., Buschmann, D., Byrd, J. B., Casert, C., Cheng, L., Cmoch, A., ... Hendrix, A. (2017). EV-TRACK: Transparent reporting and centralizing knowledge in extracellular vesicle research. *Nature Methods*, 14(3), 228–232. <https://doi.org/10.1038/nmeth.4185>
- Van Deun, J., Roux, Q., Deville, S., Van Acker, T., Rappu, P., Miinalainen, I., Heino, J., Vanhaecke, F., De Geest, B. G., De Wever, O., & Hendrix, A. (2020). Feasibility of mechanical extrusion to coat nanoparticles with extracellular vesicle membranes. *Cells*, 9(8), 1797. <https://doi.org/10.3390/cells9081797>
- van de Wakker, S. I., van Oudheusden, J., Mol, E. A., Roefs, M. T., Zheng, W., Görgens, A., El Andaloussi, S., Sluijter, J. P. G., & Vader, P. (2022). Influence of short term storage conditions, concentration methods and excipients on extracellular vesicle recovery and function. *European Journal of Pharmaceutics and Biopharmaceutics*, 170, 59–69. <https://doi.org/10.1016/j.ejpb.2021.11.012>
- Welsh, J. A., Goberdhan, D. C. I., O'Driscoll, L., Buzas, E. I., Blenkiron, C., Bussolati, B., Cai, H., Di Vizio, D., Driedonks, T. A. P., Erdbrügger, U., Falcon-Perez, J. M., Fu, Q. L., Hill, A. F., Lenassi, M., Lim, S. K., Mahoney, M. G., Mohanty, S., Möller, A., Nieuwland, R., ... Witwer, K. W. (2024). Minimal information for studies of extracellular vesicles (MISEV2023): From basic to advanced approaches. *Journal of Extracellular Vesicles*, 13(2), e12404. <https://doi.org/10.1002/jev2.12404>
- Yáñez-Mó, M., Siljander, P. R., Andreu, Z., Zavec, A. B., Borràs, F. E., Buzas, E. I., Buzas, K., Casal, E., Cappello, F., Carvalho, J., Colás, E., Cordeiro-da Silva, A., Fais, S., Falcon-Perez, J. M., Ghobrial, I. M., Giebel, B., Gimona, M., Graner, M., Gursel, I., ... De Wever, O. (2015). Biological properties of extracellular vesicles and their physiological functions. *Journal of Extracellular Vesicles*, 4, 27066. <https://doi.org/10.3402/jev.v4.27066>
- Yekula, A., Muralidharan, K., Kang, K. M., Wang, L., Balaj, L., & Carter, B. S. (2020). From laboratory to clinic: Translation of extracellular vesicle based cancer biomarkers. *Methods*, 177, 58–66.

SUPPORTING INFORMATION

Additional supporting information can be found online in the Supporting Information section at the end of this article.

How to cite this article: Adamo, G., Picciotto, S., Gargano, P., Paterna, A., Raccosta, S., Rao, E., Romancino, D. P., Ghersi, G., Manno, M., Salamone, M., & Bongiovanni, A. (2025). DetectEV: A functional enzymatic assay to assess integrity and bioactivity of extracellular vesicles. *Journal of Extracellular Vesicles*, 14, e70030. <https://doi.org/10.1002/jev2.70030>